Title: From teeth to pad: tooth loss and development of keratinous structures in sirenians.

Authors: Hautier, L.[1,2], Gomes Rodrigues, H.[3], Ferreira-Cardoso, S.[1], Emerling, C.A.[4], Porcher, M.-L.[1], Asher, R.[5], Portela Miguez, R.[2], Delsuc, F.[1]

Affiliations

[1]Institut des Sciences de l'Évolution, Université Montpellier, CNRS, IRD, EPHE, Montpellier 34095, France.

[2]Mammal Section, Life Sciences, Vertebrate Division, The Natural History Museum, London, UK.

[3]Centre de Recherche en Paléontologie— Paris (CR2P), UMR CNRS 7207, Muséum National d'Histoire Naturelle, Sorbonne Université, Paris, France.

[4]Biology Department, Reedley College, Reedley, CA 93654, USA.

[5]Department of Zoology, University of Cambridge, Cambridge, UK.

Abstract

Sirenians are a well-known example of morphological adaptation to a shallow-water grazing diet characterized by a modified feeding apparatus and orofacial morphology. Such adaptations were accompanied by an anterior tooth reduction associated with the development of keratinized pads, the evolution of which remains elusive. Among sirenians, the recently extinct Steller's sea cow represents a special case for being completely toothless. Here, we used μ-CT scans of sirenian crania to understand how motor-sensor systems associated with tooth innervation responded to innovations such as keratinized pads and continuous dental replacement. In addition, we surveyed nine genes associated with dental reduction for signatures of loss of function. Our results reveal how patterns of innervation changed with modifications of the dental formula, especially continuous replacement in manatees. Both our morphological and genomic data show that dental development was not completely lost in the edentulous Steller's sea cows. By tracing the phylogenetic history of tooth innervation, we illustrate the role of development in promoting the innervation of keratinized pads, similar to the secondary use of dental canals for innervating neomorphic keratinized structures in other tetrapod groups.

Keywords

Sirenians, tooth loss, keratinous pad, Steller’s sea cow, dental pseudogenes.

1. Introduction

Teeth represent one of the main diagnostic traits of jawed vertebrates (gnathostomes) and were selected very early on during their evolutionary history (around 450 mya; [1]). These complex structures have functions for object manipulation and environmental sensing. They played a key role in the diversification of feeding strategies [2] and enabled vertebrates to occupy a variety of ecological niches. Despite these pivotal functions, the dentition has been secondarily lost or significantly reduced in a number of tetrapod clades [1,3–5]. All extant avians and chelonians lack teeth, in lieu of the development of a keratinized beak [3,6–9]. Some non-avian dinosaurs, such as ceratopsians or maniraptoriforms [10,11], and non-mammalian synapsids, such as dicynodonts [12], also lost either partially or completely their teeth and developed keratinized rhamphotheca, i.e., beaks.

Although toothlessness is less common in mammals than turtles and birds, the dentition in several lineages is highly reduced or absent [13]. In these groups, secondary tooth loss or reduction are often related with specific dietary regimes, such as ant- and termite-eating (anteaters and pangolins) or filter feeding (baleen whales) [1]. As in other toothless tetrapods, mammalian tooth reduction frequently co-occurs with the development of specialized structures that replace teeth topologically and/or functionally such as baleens in cetaceans or sticky tongues and keratinous pads in anteaters [1]. However, traces of tooth development are still evident in some of these groups, as demonstrated by data from μ-CT (high-resolution computed tomography [14,15]. Furthermore, internal structures related to tooth development, such as nerves and blood vessels, comprise indirect evidence of how tooth development may be redeployed to serve new, specialized structures [13,16].

The evolution of the dentition, particularly when teeth are reduced or lost, is also quantifiable in a genomic context. When the selective pressure on teeth is relaxed, certain genes underlying the development of enamel and dentin can degrade into pseudogenes, characterized by various inactivating

mutations, including frameshift indels, premature stop codons, and splice site mutations. Subsets of these dental genes have been characterized as pseudogenes in enamelless mammals (e.g., aardvarks, armadillos, sloths) and edentulous tetrapods (e.g., baleen whales, anteaters, pangolins, birds, turtles) [3,4,17–20], pointing to their specific requirements in odontogenesis. Inactivation of these genes is also associated with congenital diseases in humans, particularly amelogenesis imperfecta and dentinogenesis imperfecta, and similar phenotypes in mouse models [21]. This provides a clear genotype–phenotype link when these genes become dysfunctional.

Sirenians provide a compelling example of gradual tooth loss over deep time. Living sirenians (i.e. manatees and dugongs) comprise only four species restricted to tropical and subtropical regions. By contrast, their fossil record is rich and traces back to the early middle Eocene (~55 Mya, [22]). Sirenian adaptation to a shallow-water grazing diet is characterized by a modified feeding apparatus and orofacial morphology [23–27]. Such modifications were accompanied by the acquisition of unique muscular-vibrissal complexes, combined with an anterior tooth reduction associated with the presence of shallow empty pits, long assumed to represent vestigial incisor and canine alveoli [27,28]. These pits are covered by masticatory horny pads, i.e. keratinized plates showing large abrasive surfaces that are mainly involved in the food mastication in the oral cavity [27,29]. These pads are common to all four recent species, but was especially pronounced in the recently extinct Steller's sea cows, *Hydrodamalis gigas*, which possessed completely edentulous jaws. In an opposite evolutionary trend, manatees have developed a long row of six to eight molars that exhibit a constant addition of supernumerary teeth at the back of the jaw, which then migrate anteriorly [25,30–32].

Here, we aim to understand how motor-sensorial systems associated with tooth innervation responded to innovations such as the highly developed vibrissal complex, tooth loss and replacement by thick keratinized pads, and continuous dental replacement. We used μ-CT scans of the skull of extant

and extinct sirenians to investigate the morphology of the mandibular and superior alveolar canals as osteological proxies of tooth innervation, and to understand the correlation between the evolution of sirenian orofacial anatomy and tooth reduction. To further explore the degree of dental regression in sirenians, we determined the functionality of nine genes whose proteins are tied to tooth development and maintenance. Tracing the phylogenetic history of tooth innervation enabled us to shed light on the way tooth development can promote the innervation and somatosensory role of evolutionary novelties such as horny pads, as well as reveal how nerve branching patterns changed with modifications of the dental formula, especially manatee continuous dental replacement.

2. Results

Variation of dorsal canaliculi in extant species - We investigated three-dimensional (3D) models of the mandibles, teeth, and mandibular canals of all modern sirenian species (Figs. 1 and 2). The roots of sirenian molars are particularly long, so that the innervation occasionally passes directly from the mandibular canal to the alveolus without passing through a minute canal, here defined as canaliculus. However, manatees and dugongs also display several groups of distinct dorsal canaliculi, which provide passage for vessels and nerves that nourish and innervate the teeth. The most anterior grouping is thick and formed of numerous canaliculi, some of which also connect to tooth alveoli. In the posterior area of the mandible, canaliculi run either from the mandibular canal directly to the teeth or connect several alveoli to each other (Figs. 1, 2, S2, and S3). In *T. manatus*, two to three thick canaliculi diverge anteriorly, and then separate into four or five ramifications at the level of the symphyseal pad (Figs. 1, 2, and S2). In the tooth row area, the canaliculi are thin and antero-dorsally oriented. In *T. inunguis*, up to seven anterior canaliculi were identified, which constitutes the largest number in our sample. In the tooth row area, the dorsal canaliculi are straight and dorso-ventrally oriented below the most anterior

teeth; they are more antero-dorsally oriented in the posterior part of the mandible (S2). In *T. senegalensis*, a single thick anterior branch diverges from the mandibular canal to then split into five smaller branches. Posteriorly to these branches, a canaliculus is also oriented dorso-posteriorly and is connected to the first tooth alveolus (S2). Below the tooth row, several canaliculi are clearly connected to dental roots, the most posterior ones being longer and more inclined antero-dorsally. In the only specimen of a fetal manatee in our sample (Figs. 1 and S4), vestigial teeth are present in the anterior part of both hemimandibles, with a few dorsal canaliculi being distinguishable in the posterior part of the dental pad. The low degree of ossification of the mandible at this ontogenetic stage partly prevents any clear recognition of posterior canaliculi except in the most posterior part of the tooth row. In dugongs, the anterior canaliculi usually derive from three main branches (Figs. 1, 2, and S3). Behind the symphysis in all specimens, an isolated dorsal canaliculus bifurcates into one branch that opens into the more posterior part of the pad and another branch that connects to the first dental alveolus (Figs. 1 and 2). More posteriorly, an intricate network of canaliculi connects the mandibular canal to the dental alveoli or the alveoli to each other, except for the most distal dental locus that usually connects directly to the mandibular canal. In our single specimen of a fetal dugong, several dorsal canaliculi are clearly identifiable (Figs. 1 and S4). The four anteriormost ones are each closely associated with four shallow pits, which would be covered by the dental pad in adults. Two of these dorsal canaliculi, the most anterior and posterior ones, were found in association with vestigial tooth loci on both hemimandibles (Figs. 1 and S4). An individualized dorsal canaliculus is located just posteriorly to these anterior canaliculi; this canaliculus is associated with the anteriormost premolar alveolus where no tooth is yet mineralized.

Variation of dorsal canaliculi in extinct species - All fossil taxa in our sample (*Libysiren sickenbergi*, *Prorastomus sirenoides, Halitherium taulannense*, *Rytiodus capgrandi*, and *Eosiren libyca*) showed more complete dental formulae than extant species. Also in our sample is the geologically oldest species with continuous dental replacement, *Ribodon limbatus*, which has at least six functional molars [30]. Stem sirenians were characterized by the following dental formula: I 3/3, C 1/1, P 5/5, M 3/3. Their dental formulae depart from those of manatees and dugongs, which completely lack lower incisors and canines and have lost numerous cheek teeth. Dorsal canaliculi were hard to delineate in *Prorastomus* as its mandibles are characterized by large spongiosa (Figs. 3 and S5). All the identified canaliculi associated with premolar and molar loci were dorso-ventrally oriented, joining the main mandibular canal to the roots of the cheek teeth. On the left mandible (S5) an anterior dorsal canaliculus associated to an incisor locus was also recognizable. Although both specimens of *Libysiren sickenbergi* lacked complete teeth, they showed a number of dorsal canaliculi clearly linking the mandibular canal to some empty alveolar sockets (Figs. 3 and S5). All of these canaliculi are relatively straight and antero-dorsally oriented in the anterior part of the mandible; they are more postero-dorsally oriented in its posterior part. No dorsal canaliculi are visible in the posterior part of the cheek tooth row in one specimen (NHMUK M82429); a few are recognizable in the other one (NHMUK M45675b). Dorsal canaliculi are clearly recognizable in our single specimen of *Eosiren libyca* (Figs. 3 and S5). They are divided into two clusters: one anterior grouping composed of thick canaliculi reaching empty dental alveoli dorsally, and one posterior grouping composed of thinner canaliculi connecting the mandibular canal to the roots of the cheek teeth. Most of these canaliculi are slightly antero-dorsally oriented. In *Halitherium taulannense* (Figs. 3 and S5), dorsal canaliculi are poorly distinguishable in the posterior part of the mandible. Several thin canaliculi are associated with the first premolars, while thick canaliculi are connected to empty dental alveoli in the anterior part of the jaw. *Rytiodus capgrandi*

displays a pattern very similar to that of extant dugongs, with dorsal canaliculi directly connected to the cheek teeth, which are much larger; the anterior part of the specimen is slightly damaged but the rooting of the anterior dorsal canaliculi could still be observed. The only hemi-mandible of *Ribodon limbatus* (a manatee close relative) completely lacks teeth but displays identifiable tooth alveoli as well as a high number of dorsal canaliculi. The most anterior canaliculi are slightly postero-dorsally oriented. They are followed by antero-dorsally oriented canaliculi as well as numerous posterior canaliculi, which are antero-dorsally oriented and almost horizontal. Despite being completely edentulous, *Hydrodamalis gigas* displays several distinctive dorsal canaliculi (Figs. 2, 3, and S6). Their distribution along the jaw partly mirrors that observed in toothed sirenians, especially dugongids, with anterior canaliculi joining the mandibular canal to the dental pad and posterior canaliculi opening on the dorsal surface of the mandibular horizontal ramus. The anterior canaliculi are thinner than in dugongs and manatees, and show a smaller number of ramifications. The most posterior canaliculi are curvilinear, first antero-dorsally oriented in their ventral part and postero-dorsally oriented in their dorsal part. The most posterior canaliculus is very distinctive for originating far posteriorly and extending anteriorly horizontally to the mandibular canal.

Genetic results - In the sirenians that retain teeth, we were able to recover the entire coding sequence for each of the nine dental genes in the *Trichechus manatus* and two dugong individuals. The lone exception was the middle portion of the repeat-rich 4th exon of *DSPP* in the dugong genome assemblies, which was difficult to assemble. Furthermore, we ignored exons 7–9 in *AMBN* due to their duplication in humans [33] and consequently uncertain homology. All genes appear functionally intact in these three assemblies, with one exception. *ACP4* in *Dugong* looks intact in one individual (BMBL01), but a second individual (CAJQER01) has a 1-bp (base pair) insertion just 14-bp upstream of

184 the stop codon (Figure 4). This insertion is an extra G in a string of seven G's (eight total), causing a
185 frameshift that results in the next stop codon appearing 275-bp downstream of the ancestral stop codon.
186 The validity of this insertion was tested by mapping reads to a 101-bp fragment encompassing the
187 insertion. Out of 34 mapped short reads (S7), seven have the extra G (eight total), one has two extra G's
188 (nine total), and the remaining 26 do not possess an insertion (seven total). While this variation in the
189 short reads may be indicative of a polymorphism, it is perhaps better explained as the result of
190 sequencing errors. Sampling more dugong individuals should clarify this issue. Finally, of potential
191 significance, two *DSPP* sequences were found spread across four contigs of the CAJQER01 assembly.
192 Whether this is simply an assembly artifact or evidence of a recent gene duplication is unclear and
193 warrants further investigation, particularly if there are functional consequences to possessing two *DSPP*
194 paralogs.

195 In contrast to the manatee and dugong, we found evidence of multiple dental pseudogenes in the
196 Steller's sea cow. We recovered the entire coding sequences for all genes except a few small portions:
197 15-bp in exon 5 of *AMBN*, the 3' end of exon 4 in *DSPP*, and the last 2-bp of exon 5 in *ODAM*. Among
198 the nine genes we examined, *ACP4*, *AMBN*, *ENAM*, *MMP20*, and *ODAM* show evidence suggestive of
199 pseudogenization (Fig. 4). *ACP4* has a 1-bp insertion in exon 4 (supported by 12/12 short reads) and
200 *AMBN* possesses a premature stop codon 42-bp upstream of the ancestral stop codon (25/26 short reads)
201 (S7). In *ENAM*, we found a splice acceptor mutation in intron 2 (AG → CG), which was previously
202 reported by Springer et al. [5], suggesting that this mutation may have been fixed in this species. For
203 *ODAM*, the coverage depth is quite poor for the putative mutations. Indeed, most of the gene was not
204 found in the assembly itself (7/10 exons), and had to be constructed by mapping reads to a dugong
205 reference. However, we found evidence for three inactivating mutations: exon 4 has a 1-bp deletion (4/4

206 short reads), intron 4 has a potentially polymorphic splice acceptor mutation (AG → GG) (3/5 short
207 reads), and exon 10 has a 2-bp deletion (1/1 short reads) (S7).

208 The functional status of the last potential pseudogene, *MMP20*, is more complicated. The
209 assembly's contigs are suggestive of two inactivating mutations that would render the gene
210 dysfunctional. The first starts at the the 3' end of exon 2. Rather than 9-bp followed by the splice donor
211 and the rest of the intron, there is 154-bp of a nonhomologous sequence that does not align to any of the
212 other three sirenian *MMP20* orthologs. Given that this gene is otherwise highly conserved in all three
213 species, it would suggest that this is a large insertion. Though short reads seem to support the exon 2
214 mutation when mapping to the *Hydrodamalis gigas* contig, mapping to the *Dugong dugon* contig
215 reconstructed a fully intact exon 2. The second putative mutation is a large deletion (699-bp) that
216 encompasses much of intron 7 and the 5' end of exon 8. However, a separate contig encompasses much
217 of the deleted portion, potentially suggesting an assembly error. Whereas mapping to a *D. dugon*
218 reference reconstructed an intact exon 8, with 100 short reads spanning the region right where the
219 deletion would end, mapping to the *H. gigas* reference resulted in 54 short reads supporting the validity
220 of this mutation (S8). These results may indicate that there were both functional and pseudogenic
221 *MMP20* alleles in Steller's sea cows. Alternatively, there may have been a gene duplication followed by
222 pseudogenization. Given that this is difficult to interpret with a discontiguous genome assembly, the
223 sampling of more Steller's sea cow individuals is warranted.

224

225 **3. Discussion**

226 *Sirenian tooth loss in deep time* - In most mammals, dental roots are elongate and tooth alveoli
227 open directly into the mandibular canal [13]. In species with a reduced dentition, the link between the
228 main mandibular canal and the teeth is maintained via the development of an intricate network of dorsal

canaliculi [13]. Our observations on sirenians confirm the existence of a link between the presence of teeth and the development of dorsal canaliculi. On the one hand, fossil species with a full (or nearly so) dental formula usually display dorsal canaliculi directly connected to tooth alveoli. On the other hand, extant manatees and dugongs show dorsal canaliculi linked to their remaining cheek teeth. Dental reduction occurs during growth in dugongs, with only two to three molars observed in old adult individuals. We observed that, for some dental loci (i.e., premolars) that are rapidly lost, the associated dorsal canaliculi persist throughout development and into adulthood (Figs 1D and 2B).

Extant sirenian species also display some anterior dorsal canaliculi with no apparent connection to tooth alveoli. These canaliculi are connected to pairs of shallow pits covered by the dental pad that can contain non-erupting vestigial teeth in adult specimens [27,28]. We argue that all these shallow pits actually represent true dental alveoli and host several vestigial teeth that are expressed and then resorbed in fetal stages (Figs. 1 and S4). Reconstructions of dental formulae of fossil taxa based on empty anterior alveoli are therefore not straightforward, as such pits could be misinterpreted as alveoli hosting functional teeth, with the development of the keratinous pad being potentially overlooked in some stem sirenians. Dugongs often develop vestigial teeth ventral to the keratinised pad (S3, E and H, [27]). When present, these vestigial teeth were systematically associated with an individual anterodorsal canaliculi that contacts the tooth alveolus before reaching the bone surface (S3, E and H).

In the anterior part of the mandible of manatees and dugongs, the distribution of dorsal canaliculi roughly coincides with the pattern observed in stem sirenians (Fig. 3), which typically have three incisors and one canine. In humans, the innervation of incisors and canines starts from a thick common branch that diverges from the main nerve, before splitting into thinner canals to innervate the tooth loci [34]. The larger the nerve spindle, the greater the sensitivity, which implies that anterior teeth likely require substantial vascularisation and innervation. This pattern may be analogous to the thick anterior

252 branch of extant sirenians that innervates their keratinised plate through shallow pits [35]. We propose
253 that the anterior distribution of dorsal canaliculi in extant sirenians matches that of vestigial tooth loci,
254 as suggested by our prenatal data (Figs. 1 and S4), and that dental innervation is retained after tooth
255 resorption. The number of anterior dorsal canaliculi only roughly coincides with the sirenian ancestral
256 dental formula, which includes three incisors and one canine (Fig. 3). In dugongs, the anterior dorsal
257 canaliculi consistently derive from three main branches that can be multifurcated, but the number of
258 branches appears more variable in manatee species. An excessive number of branches compared to the
259 number of teeth may be explained by variation in the bifurcation pattern of nerves as previously
260 observed in humans [34], both intraspecifically and individually. The absence of bifurcations in fetuses
261 (Figs. 1 and S4) and their limited development in juvenile specimens (S2, A and D; S3, A-D) might
262 suggest that these bifurcated patterns actually develop along with bone, later during development.

263

264 *A path through edentulism* - The internal anatomy of partially or completely toothless sirenians
265 shows that they retained dental structures allowing for the passage of nerves and blood vessels, i.e.,
266 dorsal canaliculi. We think these are vestiges of actual tooth loci [13]. In humans, the development of
267 loci on the dental lamina is accompanied by a projection of a branch complex from the inferior alveolar
268 nerve [34]. The development of the neurovascular network occurs during the first two stages of tooth
269 development (initiation and budding; see [36]). Human tooth nerve bundles are retained after tooth loss
270 induced by senescence [37]. Ferreira-Cardoso et al. [13] proposed that tooth development maintains the
271 innervation and irrigation of the dorsal margin of the mandible in toothless mammals such as baleen
272 whales and anteaters. *Hydrodamalis gigas* was completely edentulous but still displayed an innervation
273 pattern that resembled that of extant toothed sirenians, with thick anterior canaliculi joining the
274 mandibular canal to the dental pad and posterior canaliculi opening on the dorsal surface of the

mandible. This suggests that the developmental program for tooth development is not lost in Steller's sea cows, as previously proposed by Nordmann [38], Murie [39], and Woodward [40].

Consistent with the morphological evidence of dental regression, elements of several genes were disabled in the edentulous Steller's sea cow. All of the inactivated genes (*ACP4*, *AMBN*, *ENAM*, *ODAM*) encode proteins expressed in ameloblasts during enamel development [41], with two specifically involved in forming the protein matrix laid down during amelogenesis (*AMBN*, *ENAM*). One of the proteins (ODAM) continues to be expressed in the junctional epithelium [41,42], likely contributing to the tight seal between the teeth and the gingiva. Notably, neither a gene tied to dentin formation (*DSPP*) and tooth loss (*ODAPH*) [17,43] lacked evidence for pseudogenization, suggesting that the genetic potential for developing teeth with dentin, possibly covered by weak enamel, may have been retained in *Hydrodamalis*.

Compared to other edentulous vertebrates, the genetic repertoire for tooth development in Steller's sea cow appears relatively intact. In addition to having only a few genes clearly pseudogenized, there is a paucity of accumulated inactivating mutations. By contrast, among placental mammals, baleen whales (Mysticeti) [4,20], anteaters (Vermilingua) [17] and pangolins (Pholidota) [44] have more depleted sets of dental genes, typically with far more inactivating mutations. For instance, all nine genes are inactivated in anteaters. Whereas the Steller's sea cow has a single inactivating mutation in *ENAM*, over 40 have been reported for *ENAM* in the silky anteater (*Cyclopes didactylus*)[17]. Similarly, the dugong [27], which presents a thin layer of enamel worn shortly after eruption, shows no unambiguous evidence of pseudogenization in its set of dental genes. This contrasts with the long-nosed armadillos (Dasypodidae), which similarly have simplistic teeth with thin enamel that wears away early in development. All dasypodids possess pseudogenized orthologs of *ACP4*, *AMTN* and *ODAM*, with some species variably presenting evidence of inactivated *ENAM*, *AMBN* and *MMP20* [17].

Two factors that may explain this contrast in pseudogenization patterns include the timing of tooth loss and the tempo of evolution. Being large-bodied mammals with long generation times, elevated longevity, and small population sizes, sirenians have a low rate of evolution, which leads to a decreased nucleotide substitution rate [45–48]. As such, frameshift indels, premature stop codons and other such mutations would presumably be fixed at a slow rate, especially if these genes are under relaxed selection. The polymorphic inactivating mutations described here would be consistent with this hypothesis, under the assumption that they are drifting and not yet at fixation. If edentulism is recent, there should be correspondingly fewer inactivating mutations. Fossil evidence suggests that the lineage leading to the Steller's sea cow lost teeth relatively recently. The edentulous *Hydrodamalis cuestae* and toothed *Dusisiren* spp. [49] are the Steller's sea cow's closest known relatives, successively, based on two large sirenian phylogenetic datasets [5,22]. Whereas *Dusisiren* spp. ranged from approximately 16 to 5.3 million years ago (mya), the earliest *H. cuestae* specimen was described in the Tortonian (11.6–7.2 mya) [50]. By contrast, anteaters began a process of dental regression roughly 58 mya which led to complete tooth loss about 38 mya [17], and even slowly evolving mysticetes began losing enamel perhaps as early as 35 mya before becoming edentulous 26–20 mya [51][4]. Future work that could help clarify the genomic basis of dental erosion in these species includes detailed molecular evolutionary analyses, sampling from multiple Steller's sea cow and dugong individuals, and exploring patterns of evolution in non-coding regulatory regions associated with tooth formation.

From dental reduction to continuous dental replacement. The continuous dental replacement represents a morphological innovation documented in extant manatee species [25,30,32,52]. Continuous replacement represents a morphological characteristic common to most trichechines, including the late Miocene *Ribodon* [30,53], which is absent in the early diverging *Potamosiren* that displayed a reduced

adult dentition (*i.e.*, two to three molars; [30,52]). This peculiar mode of tooth replacement represents an evolutionary convergence likely related to the ingestion of abrasive and tough items [30,31]. Both sirenian evolutionary trends towards dental reduction and continuous dental replacement are tightly related to different dietary properties, mostly soft seagrasses for the former and abrasive, fibrous freshwater plants for the latter [30,54]. An important wear gradient has been observed in many sirenians, in association with anterior tooth loss during ontogeny, meaning that the eruption of posteriormost molars is likely delayed and then supplemented by a mesial drift (i.e. anterior migration) of teeth.

The anterior movement of dental roots during growth is allowed by combination of constant alveolar bone resorption and apposition [31], and remodeling of the periodontal ligament [55], but we did no observe any disruption of dorsal canaliculi. Such dental drift could explain the anterior tilt of the posterior dorsal canaliculi observed in adults, and is consistent with the fact that juvenile specimens display straighter anterior dorsal canaliculi. This orientation might then constitute a new feature defining the intensity of the drift, a nearly horizontal orientation of dorsal canaliculi defining a strong or continuous dental drift (sensu [31]). The pattern of dorsal canaliculi observed in *Ribodon* would then be in line with previous propositions that continuous replacement evolved from the Late Miocene onward in trichechids [30]. A moderate drift of distal molars was also described in modern dugongids (*i.e.* dugong and *Metaxytherium* species; [27,56], inducing the loss of premolars and first molars. Accordingly, we observed an anterior tilt of dorsal canaliculi for most cheek teeth during dugong growth, but these canaliculi are shorter and more curved than in trichechids. Such a tilted pattern is also present in extinct dugongids, especially *Rytiodus*, implying that dental drift and associated delayed eruption probably appeared early in sirenians.

343 *Convergent redeployment of tooth developmental pathway for keratinized structures* - In
344 mammals, dental innervation has a sensory role [57]. Following the discovery of a new sensory organ in
345 living mysticetes [58], Peredo et al. [59] proposed a mechanoreceptive-related role for dorsal canaliculi
346 in mysticetes, with the retention of canaliculi contributing to the control of rotation of the hemi-
347 mandibles, which are unfused. A similar sensorial role was hypothesized in toothless anteaters [13], with
348 the canaliculi putatively allowing the coordination between the protractile tongue and the two halves of
349 the jaw, which are also unfused. In sirenians, the canaliculi probably do not provide a function in
350 intramandibular coordination since their symphysis is fused and their hemi-mandibles cannot move
351 independently. Manatees and dugongs have vibrissae distributed in an arc around the keratinised pad
352 and on the lips. These vibrissae are used to collect and position food between the plates [60]. Seagrass is
353 then broken down mechanically by the upper and lower keratinised plates during transit to the jugal
354 teeth [27,29]. The crushing provided by the oral plates partially or completely compensates for the small
355 number of teeth in dugongs. This anatomical complex forms an efficient collection, transport, and
356 chewing system, which combines mechanical and sensory roles [60]. In fact, considering their small
357 gape and the lack of cheek pouches, Lanyon et al. [27] expressed doubt that dugongs could actually use
358 their teeth for chewing their food inside their mouth cavity. These hindgut fermenters would instead
359 mainly use their keratinised pads, which are better adapted for processing rapidly large quantities of low
360 fibre seagrass.

361 A close relationship between tooth development and the evolution of keratinized innovations of
362 the feeding apparatus was proposed in several toothless mammals [1,14,15,61]. In cetaceans, several
363 studies [62,63] proposed that the neurovascular anatomy of the upper teeth was co-opted for nourishing
364 baleen. Lanzetti [14] showed that baleen rudiments develop alongside tooth germs within the alveolar
365 canals of minke whales. Thewissen et al. [15] demonstrated that some signaling proteins are involved in

366 both tooth and baleen formation in bowhead whales, so that early tooth development constitutes a
367 prerequisite to baleen development, as baleen is vascularized from the same artery that irrigates vestigial
368 teeth [61,63]. Myrmecophagous xenarthrans have tooth remnants in the form of dorsal canaliculi, which
369 were proposed to enable the innervation and vascularization of a mandibular keratinized pad [13]. In
370 platypuses, milk teeth are rapidly lost after birth at weaning time and replaced by horny pads, which are
371 used for food processing [64,65]. In dugongs, we showed that the canaliculi located just posterior to the
372 symphyseal area supply both the horny pad and the first dental alveolus. We presented ontogenetic,
373 paleontological, and genetic evidence for commonalities between the developmental programs for teeth
374 and keratinous pads. Lanyon et al. [27] noted that the occlusion of the lower and upper dental pads and
375 the occlusion of lower and upper cheekteeth occur simultaneously. We propose that the ascending
376 branches of the inferior alveolar nerve might be part of the somatosensory system involved in
377 mechanoreception, as such integrated movement would require a tactile feedback originating from the
378 dorsal margin of the mandible. Following this hypothesis, the dental sensory receptors that project via
379 the inferior alveolar nerve would were co-opted to confer a somatosensory role to the mandibular
380 keratinized pad.

381

382 **4. Conclusion**

383 The evolution of alternative feeding systems to teeth has long attracted attention of biologists
384 [6,7,14,59,61,66]. In birds, the intricate relationships between tooth loss and the development of
385 keratinized beaks was hypothesized to be due either to physical constraints on tooth initiation, the early
386 interruption of odontogenesis being initiated by the development of the keratinous ramphoteca [6], or to
387 pleiotropic effect of genes involved in both rhamphotheca development and tooth pathway signaling
388 (*e.g.*, *BMP4*; [67,68]). This trend was supported, in part, by the bird fossil record showing the expansion

389 of a keratinized rostrum associated with a reduced tooth number [6,69] or with the replacement of
390 portions of the dental rows by a beak during the ontogeny of ceratosaurian theropods [10].
391 Odontogenesis disruption might indeed be triggered by the early keratinisation of pads and beaks in
392 mammals and birds, respectively. However, Wang et al. [10,11] studied alveolar vestiges conserved in
393 the interior of the jaws of beaked theropod dinosaurs *Limusaurus*, whose juveniles develop teeth that are
394 replaced by a beak in adults. They showed that tooth alveoli in some edentulous dinosaurs are recycled
395 to improve the neurovascularisation of the mandible and are partially modified into structures that serve
396 to innervate and irrigate the beak. We think that the pattern of innervation of the keratinous pad in
397 sirenian resembles that of these *Limusaurus* beaks. Using a long and slow developmental process such
398 as tooth development might constitute a simple way for maintaining the dorsal innervation of keratinous
399 structures in order to preserve sensorial functions of the alveolar region, even while some selective
400 pressures later induced tooth loss [13]. Sirenians constitute a further example of a secondary use of
401 dental canals for innervating novel keratinized structures.

402

403 **5. Materials and methods**

404 *Morphological data* - We describe the mandibular canals of the four extant sirenian species: *Trichechus*
405 *inunguis*, *T. manatus*, *T. senegalensis*, and *Dugong dugon*. We also included seven key extinct taxa:
406 *Prorastomus sirenoides* (lower Lutetian), *Libysiren sickenbergi* (lower Lutetian), *Halitherium*
407 *taulannense* (Priabonian), *Eosiren libyca* (Priabonian), *Rytiodus capgrandi* (lower Miocene), *Ribodon*
408 *limbatus* (Late Miocene), and *Hydrodamalis gigas* (Steller's sea cow, extinct since the 18th century).
409 Mandibles were chosen to study dental innervation patterns because they are composed of a single bone
410 enclosing the inferior alveolar nerves and arteries. The 47 specimens belong to the following collections:
411 Natural History Museum, London (NHMUK); Muséum National d'Histoire Naturelle, Paris (MNHN);

412 Muséum d'Histoire Naturelle de Toulouse, Toulouse (MHNT); University Museum of Zoology,
413 Cambridge (UMZC); the Institut Royal des Sciences Naturelles de Belgique, Brussels (IRSNB); Institut
414 des Sciences de l'Evolution, Uniersity of Montpellier (UM). High-resolution microtomography (μCT)
415 was performed at Montpellier Rio Imaging (MRI) platform, the Imaging Analysis Center (NHMUK),
416 the Cambridge Biotomography Centre, and the AST-RX platform (MNHN) with different resolutions
417 (S1-6) The left hemi-mandibles (the right one was used if the left one was missing or broken) were
418 reconstructed, with respective mandibular canals and teeth. Avizo 2022.1 was used to perform the 3D
419 reconstructions and measurements. The virtually restored 3D models are deposited in MorphoMuseuM
420 [70]. Two ontogenetic stages were identified and distinguished: juveniles still presenting deciduous
421 premolars, and adults bearing only molars in manatees and dugongs [25,27].

422

423 *Genetic data* - We obtained nine core dental genes from *Trichechus manatus*, *Dugong dugon*,
424 and *Hydrodamalis gigas*. These were *ACP4* (acid phosphatase 4), *AMBN* (ameloblastin), *AMELX*
425 (amelogenin), *AMTN* (amelotin), *DSPP* (dentin sialophosphoprotein), *ENAM* (enamelin), *MMP20*
426 (metalloproteinase 20), *ODAM* (odontogenic, ameloblast-associated), and *ODAPH* (odontogenesis-
427 associated phosphoprotein). We first obtained human orthologs for each gene using mRNA transcripts
428 deposited in GenBank. Next, we searched each gene against the manatee assembly (GCF_000243295.1)
429 in NCBI's RefSeq database using discontiguous megablast. We downloaded the whole genes for each
430 positive blast result and imported them into Geneious Prime [71]. Any long strings of N's were reduced
431 to ~10 to prevent complications in sequence alignments. Next, we used the manatee sequence to search
432 against two dugong assemblies (WGS projects BMBL01 and CAJQER01) and one Steller's sea cow
433 assembly [72] in NCBI's whole genome shotgun contig database using discontiguous megablast. We
434 next imported the matching sequences into Geneious and aligned all sequences using MUSCLE [73].

We examined each alignment by eye and adjusted them manually when likely nonhomologous bases were erroneously aligned (SI Dataset). Non-coding exons were deleted when present, since our focus was on coding sequences only. As such, our exon numbering only pertains to coding exons. Finally, we examined each sequence for frameshift indels, premature stop codons, and variations in splice sites, and start and stop codons. As the Steller's sea cow genome assembly is relatively discontiguous (genome coverage = 11x, contig N50 = 1,345, scaffold N50 = 1,430), in some cases we needed to fill in gaps in the coding sequence and to validate putative inactivating mutations. We thus downloaded short reads from the NCBI Sequence Read Archive [74] and mapped them to the assembled gene sequences using the short read settings (-ax sr) of Minimap2 [75]. We used the dugong as a reference for gap filling, and the Steller's sea cow sequences as references for validating mutations. We examined the resulting mapping files by eye in Geneious Prime and adjusted the reference length when there were excessive mapped reads due to repetitive regions in the target sequence (Supplementary SI Dataset).

Acknowledgements

We are grateful to Peter Giere and Frieder Mayer (Museum für Naturkunde, Berlin), Guillaume Billet and Claire Sagne (Museum National d'Histoire Naturelle, Paris), Pip Brewer (Natural History Museum, London), Georges Lenglet (Institut Royal des Sciences Naturelles de Belgiques, Brussels), Yves Laurent (Museum d'Histoire Naturelle de Toulouse), Anne-Lise Charruault (Institut des Sciences de l'Evolution de Montpellier) and their colleagues for access to comparative material. We thank N. Burma for his support with specimen selection. We are grateful to Vincent Fernandez (NHMUK), Marta Bellato (AST-RX platform, UAR 2700 2AD CNRS-MNHN, Paris), and Renaud Lebrun (ISEM/MRI platform) for their assistance with μ-CT scanning. S.F.-C., L.H. and F.D. were supported by a European Research Council (ERC) consolidator grant (ConvergeAnt #683257). S.F.C. benefitted from the

SYNTHESYS Project (Project GB-TAF-2424) founded by the European Community Research Infrastructure Action under the FP7 Integrating Activities Programme. L.H. and F.D. were supported by Centre National de la Recherche Scientifique (CNRS). This work has been supported by "Investissements d'Avenir" grants managed by Agence Nationale de la Recherche Labex CEMEB (ANR-10-LABX-0004), Labex NUMEV (ANR-10-LABX-0020), and Labex CEBA (ANR-10-LABX-0025). We thank Mark S. Springer and Kevin L. Campbell for helpful discussions. We also thank two anonymous reviewers as well as John Hutchinson for their comments, which help improving this manuscript. This is a contribution ISE-M 2023-234 of the Institut des Sciences de l'Evolution de Montpellier.

References

1. Davit-Béal, T., Tucker, A. S. & Sire, J. Y. 2009 Loss of teeth and enamel in tetrapods: Fossil record, genetic data and morphological adaptations. *J. Anat.* **214**, 477–501. (doi:10.1111/j.1469-7580.2009.01060.x)

2. Berkovitz, B. & Shellis, P. 2018 *The teeth of mammalian vertebrates.* Academic P.

3. Meredith, R. W., Zhang, G., Gilbert, M. T. P., Jarvis, E. D. & Springer, M. S. 2014 Evidence for a single loss of mineralized teeth in the common avian ancestor. *Science (80-.).* **346**, 1254390.

4. Randall, J. G., Gatesy, J. & Springer, M. S. 2022 Molecular evolutionary analyses of tooth genes support sequential loss of enamel and teeth in baleen whales (Mysticeti). *Mol. Phylogenet. Evol.* **171**, 107463. (doi:10.1016/j.ympev.2022.107463)

5. Springer, M. S. et al. 2015 Interordinal gene capture, the phylogenetic position of Steller's sea cow based on molecular and morphological data, and the macroevolutionary history of Sirenia.

480 *Mol. Phylogenet. Evol.* **91**, 178–193. (doi:10.1016/j.ympev.2015.05.022)

481 6. Louchart, A. & Viriot, L. 2011 From snout to beak: The loss of teeth in birds. *Trends Ecol. Evol.*
482 **26**, 663–673. (doi:10.1016/j.tree.2011.09.004)

483 7. Wang, S. H. U. O., Stiegler, J. O. S. E. F., Wu, P. & Chuong, C. M. 2020 Tooth vs. beak: the
484 evolutionary developmental control of the avian feeding apparatus. In *Pennaraptoran Theropod*
485 *Dinosaurs: Past Progress and New Frontiers* (eds M. PITTMAN & X. XU), pp. 205–228. New-
486 York: Bulletin of the American Museum of Natural History.

487 8. Tokita, M., Chaeychomsri, W. & Siruntawineti, J. 2013 Developmental basis of toothlessness in
488 turtles: Insight into convergent evolution of vertebrate morphology. *Evolution (N. Y).* **67**, 260–
489 273. (doi:10.1111/j.1558-5646.2012.01752.x)

490 9. Meredith, R. W., Gatesy, J. & Springer, M. S. 2013 Molecular decay of enamel matrix protein
491 genes in turtles and other edentulous amniotes. *BMC Evol. Biol.* **13**, 20. (doi:10.1186/1471-2148-
492 13-20)

493 10. Wang, S., Stiegler, J., Amiot, R., Wang, X., Du, G. hao, Clark, J. M. & Xu, X. 2017 Extreme
494 ontogenetic changes in a ceratosaurian theropod. *Curr. Biol.* **27**, 144–148.
495 (doi:10.1016/j.cub.2016.10.043)

496 11. Wang, S., Zhang, Q. & Yang, R. 2018 Reevaluation of the dentary structures of caenagnathid
497 oviraptorosaurs (Dinosauria, Theropoda). *Sci. Rep.* **8**, 1–9. (doi:10.1038/s41598-017-18703-1)

498 12. Kammerer, C. F., Angielczyk, K. D. & Fröbish, J. 2011 A comprehensive taxonomic revision of
499 Dicynodon (Therapsida, Anomodontia) and its implications for dicynodont phylogeny,
500 biogeography, and biostratigraphy. *J. Vertebr. Paleontol.* **31**, 1–158.

13. Ferreira-Cardoso, S., Delsuc, F. & Hautier, L. 2019 Evolutionary Tinkering of the Mandibular Canal Linked to Convergent Regression of Teeth in Placental Mammals. *Curr. Biol.* **29**. (doi:10.1016/j.cub.2018.12.023)

14. Lanzetti, A. 2019 Prenatal developmental sequence of the skull of minke whales and its implications for the evolution of mysticetes and the teeth-to-baleen transition. *J. Anat.* **235**, 725–748. (doi:10.1111/joa.13029)

15. Thewissen, J. G. M., Hieronymus, T. L., George, J. C., Suydam, R., Stimmelmayr, R. & McBurney, D. 2017 Evolutionary aspects of the development of teeth and baleen in the bowhead whale. *J. Anat.* **230**, 549–566. (doi:10.1111/joa.12579)

16. Peredo, C. M. & Pyenson, N. D. 2021 Morphological variation of the relictual alveolar structures in the mandibles of baleen whales. *PeerJ* **9**, 1–11. (doi:10.7717/peerj.11890)

17. Emerling, C. A., Gibb, G. C., Tilak, M.-K., Hughes, J. J., Kuch, M., Duggan, A. T., Poinar, H. N., Nachman, M. W. & Delsuc, F. 2023 Genomic data suggest parallel dental vestigialization within the xenarthran radiation. *Peer Community J.* **3**, **e75**, 2022.12.09.519446. (doi:doi:10.24072/pcjournal.303)

18. Meredith, R. W., Gatesy, J., Murphy, W. J., Ryder, O. a & Springer, M. S. 2009 Molecular decay of the tooth gene Enamelin (ENAM) mirrors the loss of enamel in the fossil record of placental mammals. *PLoS Genet.* **5**, e1000634. (doi:10.1371/journal.pgen.1000634)

19. Fabre, P.-H., Hautier, L. & Douzery, E. J. P. 2015 *A synopsis of rodent molecular phylogenetics, systematics and biogeography*. (doi:10.1017/CBO9781107360150.003)

20. Springer, M. S., Emerling, C. A., Gatesy, J., Randall, J., Collin, M. A., Hecker, N., Hiller, M. &

Delsuc, F. 2019 Odontogenic ameloblast-associated (ODAM) is inactivated in toothless/enamelless placental mammals and toothed whales. *BMC Evol. Biol.* **19**, 1–19. (doi:10.1186/s12862-019-1359-6)

21. Smith, C. E. L., Poulter, J. A., Antanaviciute, A., Kirkham, J., Brookes, S. J., Inglehearn, C. F. & Mighell, A. J. 2017 Amelogenesis imperfecta; genes, proteins, and pathways. *Front. Physiol.* **8**, 435. (doi:10.3389/fphys.2017.00435)

22. Heritage, S. & Seiffert, E. R. 2022 Total evidence time-scaled phylogenetic and biogeographic models for the evolution of sea cows (Sirenia, Afrotheria). *PeerJ* **10**, 1–52. (doi:10.7717/peerj.13886)

23. Domning, D. P. 1977 Observations on the Myology of Dugong dugon (Müller). *Smithson. Contrib. to Zool.* , 68.

24. Domning, D. P. 1978 The myology of the Amazonian Manatee, *Trichechus inunguis*. *Acta Amaz.* **8**, 5–81.

25. Domning, D. P. & Hayek, L. A. C. 1984 Horizontal tooth replacement in the Amazonian manatee (Trichechus inunguis). *Mammalia* **48**, 105–128. (doi:10.1515/mamm.1984.48.1.105)

26. Marshall, C. D., Clark, L. A. & Reep, R. L. 1998 The muscular hydrostat of the Florida manatee (Trichechus manatus latirostris): a functional morphological model of perioral bristle use. *Mar. Mammal Sci.* **14**, 290–303.

27. Lanyon, J. M. & Sanson, G. D. 2006 Degenerate dentition of the dugong (*Dugong dugon*), or why a grazer does not need teeth: Morphology, occlusion and wear of mouthparts. *J. Zool.* **268**, 133–152. (doi:10.1111/j.1469-7998.2005.00004.x)

543 28. Lyman, P. 1939 A vestigial Lower Incisor in the *Dugong*. *J. Mammal.* **20**, 229–231.

544 29. Lanyon, J. M. & Sanson, G. D. 2006 Mechanical disruption of seagrass in the digestive tract of
545 the dugong. *J. Zool.* **270**, 277–289. (doi:10.1111/j.1469-7998.2006.00135.x)

546 30. Domning, D. P. 1982 Evolution of manatees : a speculative history. *J. Paleontol.* , 599–619.

547 31. Gomes Rodrigues, H., Marangoni, P., Šumbera, R., Tafforeau, P., Wendelen, W. & Viriot, L.
548 2011 Continuous dental replacement in a hyper-chisel tooth digging rodent. *Proc. Natl. Acad. Sci.*
549 *U. S. A.* **108**, 17355–17359. (doi:10.1073/pnas.1109615108)

550 32. Beatty, B. L., Vitkovski, T., Lambert, O. & Macrini, T. E. 2012 Osteological associations with
551 unique tooth development in manatees (Trichechidae, Sirenia): a detailed look at modern
552 *Trichechus* and a review of the fossil record. *Anat. Rec.* **295**, 1504–1512. (doi:10.1002/ar.22525)

553 33. Toyosawa, S., Fujiwara, T., Ooshima, T., Shintani, S., Sato, A., Ogawa, Y., Sobue, S. & Ijuhin,
554 N. 2000 Cloning and characterization of the human ameloblastin gene. *Gene* **256**, 1–11.
555 (doi:10.1093/molehr/8.6.525)

556 34. Carter, R. B. & Keen, E. N. 1971 Histology and intramandibular course of the inferior alveolar
557 nerve. *J. Anat.* **108**, 433–440. (doi:10.1007/s00784-010-0459-x)

558 35. Domning, D. P. 2022 What Can We Infer About the Behavior of Extinct Sirenians? In *Ethology*
559 *and Behavioral Ecology of Sirenia*, pp. 1–17. Springer.

560 36. Fried, K. & Gibbs, J. 2014 Dental Pulp Innervation. In *The Dental Pulp: Biology, Pathology, and*
561 *Regenerative Therapies*, pp. 75-95. Springer.

562 37. Wadu, S. G., Penhall, B. & Townsend, G. C. 1997 Morphological variability of the human
563 inferior alveolar nerve. *Clin. Anat.* **10**, 82–87.

564 38. Nordmann von, A. 1862 Beiträge zur Kenntnis des Knochen-baues der *Rhytina stelleri*. *Acta Soc.*
565 *Sci. Fenn.* **7**, 1–33.

566 39. Murie, J. 1872 V. On the Form and Structure of the Manatee (*Manatus americanus*). *Trans. Zool.*
567 *Soc. London* **8**, 127–220.

568 40. Woodward, H. 1885 IV.—On the Fossil Sirenia in the British Museum (Natural History),
569 Cromwell Road, S.W. *Geol. Mag.* **2**, 412–425. (doi:10.1017/S0016756800005616)

570 41. Ganss, B. & Abbarin, N. 2014 Maturation and beyond: proteins in the developmental continuum
571 from enamel epithelium to junctional epithelium. *Front. Physiol.* **5**, 1–6.
572 (doi:10.3389/fphys.2014.00371)

573 42. Fouillen, A., Dos Santos Neves, J., Mary, C., Castonguay, J. D., Moffatt, P., Baron, C. & Nanci,
574 A. 2017 Interactions of AMTN, ODAM and SCPPPQ1 proteins of a specialized basal lamina that
575 attaches epithelial cells to tooth mineral. *Sci. Rep.* **7**, 1–11. (doi:10.1038/srep46683)

576 43. Springer, M. S., Starrett, J., Morin, P. A., Lanzetti, A., Hayashi, C. & Gatesy, J. 2016 Inactivation
577 of C4orf26 in toothless placental mammals. *Mol. Phylogenet. Evol.* **95**, 34–45.
578 (doi:10.1016/j.ympev.2015.11.002)

579 44. Meredith, R. W. et al. 2011 Impacts of the Cretaceous Terrestrial Revolution and KPg extinction
580 on mammal diversification. *Science* **334**, 521–4. (doi:10.1126/science.1211028)

581 45. Li, W. H., Ellsworth, D. L., Krushkal, J., Chang, B. H. J. & Hewett-Emmett, D. 1996 Rates of
582 nucleotide substitution in primates and rodents and the generation-time effect hypothesis. *Mol.*
583 *Phylogenet. Evol.* **5**, 182–187. (doi:10.1006/mpev.1996.0012)

584 46. Welch, J. J., Bininda-Emonds, O. R. P. & Bromham, L. 2008 Correlates of substitution rate

variation in mammalian protein-coding sequences. *BMC Evol. Biol.* **8**, 1–12. (doi:10.1186/1471-2148-8-53)

47. Lartillot, N. & Delsuc, F. 2012 Joint reconstruction of divergence times and life-history evolution in placental mammals using a phylogenetic covariance model. *Evolution (N. Y).* **66**, 1773–1787. (doi:10.1111/j.1558-5646.2011.01558.x)

48. Latrille, T., Lanore, V. & Lartillot, N. 2021 Inferring long-term effective population size with mutation-selection models. *Mol. Biol. Evol.* **38**, 4573–4587. (doi:10.1093/molbev/msab160)

49. Kobayashi, S., Horikawa, H. & Miyazaki, S. 1995 A new species of sirenia (Mammalia: Hydrodamalinae) from the shiotsubo formation in takasato, aizu, fukushima prefecture, Japan. *J. Vertebr. Paleontol.* **15**, 815–829. (doi:10.1080/02724634.1995.10011264)

50. Domning, D. P. 1978 *Sirenian evolution in the North Pacific ocean*. University of California Press.

51. Peredo, C. M., Pyenson, N. D., Marshall, C. D. & Uhen, M. D. 2018 Tooth loss precedes the origin of baleen in whales. *Curr. Biol.* **28**, 3992-4000.e2. (doi:10.1016/j.cub.2018.10.047)

52. Suarez, C., Gelfo, J. N., Moreno-Bernal, J. W. & Velez-Juarbe, J. 2021 An early Miocene manatee from Colombia and the initial Sirenian invasion of freshwater ecosystems. *J. South Am. Earth Sci.* **109**, 103277. (doi:10.1016/j.jsames.2021.103277)

53. Domning, D. P. 2005 Fossil sirenia of the west Atlantic and Caribbean region. VII. Pleistocene Trichechus manatus linnaeus, 1758. *J. Vertebr. Paleontol.* **25**, 685–701. (doi:10.1671/0272-4634(2005)025[0685:FSOTWA]2.0.CO;2)

54. Domning, D. P. 2001 Sirenians, seagrasses, and Cenozoic ecological change in the Caribbean.

606 *Palaeogeogr. Palaeoclimatol. Palaeoecol.* **166**, 27–50. (doi:10.1016/S0031-0182(00)00200-5)

607 55. Henneman, S., Von Den Hoff, J. W. & Maltha, J. C. 2008 Mechanobiology of tooth movement.
608 *Eur. J. Orthod.* **30**, 299–306. (doi:10.1093/ejo/cjn020)

609 56. Carone, G. & Domning, D. P. 2007 *Metaxytherium serresii* (Mammalia: Sirenia): new pre-
610 Pliocene record, and implications for Mediterranean paleoecology before and after the Messinian
611 Salinity Crisis. *Boll. della Soc. Paleontol. Ital.* **46**, 55–92.

612 57. Anderson, D. J., Hannam, A. G. & Matthews, B. 1970 Sensory mechanisms in mammalian teeth
613 and their supporting structures. *Physiol. Rev.* **50**, 171–195.

614 58. Pyenson, N. D., Goldbogen, J. A., Vogl, A. W., Szathmary, G., Drake, R. L. & Shadwick, R. E.
615 2012 Discovery of a sensory organ that coordinates lunge feeding in rorqual whales. *Nature* **485**,
616 498–501. (doi:10.1038/nature11135)

617 59. Peredo, C. M., Pyenson, N. D., Uhen, M. D. & Marshall, C. D. 2017 Alveoli, teeth, and tooth
618 loss: Understanding the homology of internal mandibular structures in mysticete cetaceans. *PLoS*
619 *One* **12**, 1–26. (doi:10.1371/journal.pone.0178243)

620 60. Marshall, C. D., Maeda, H., Iwata, M., Furuta, M., Asano, S., Rosas, F. & Reep, R. L. 2003
621 Orofacial morphology and feeding behaviour of the dugong, Amazonian, West African and
622 Antillean manatees (Mammalia: Sirenia): functional morphology of the muscular-vibrissal
623 complex. *J. Zool.* **259**, 245–260. (doi:10.1017/S0952836902003205)

624 61. Ekdale, E. G., Deméré, T. A. & Berta, A. 2015 Vascularization of the gray whale palate (Cetacea,
625 Mysticeti, *Eschrichtius* robustus): soft tissue evidence for an alveolar source of blood to baleen.
626 *Anat. Rec.* **298**, 691–702. (doi:10.1002/ar.23119)

62. Gatesy, J., Ekdale, E. G., Deméré, T. A., Lanzetti, A., Randall, J., Berta, A., El Adli, J. J., Springer, M. S. & McGowen, M. R. 2022 Anatomical, ontogenetic, and genomic homologies guide reconstructions of the teeth-to-baleen transition in mysticete whales. *J. Mamm. Evol.* **29**, 891–930. (doi:10.1007/s10914-022-09614-8)

63. Ekdale, E. G. & Demé, T. A. 2022 Neurovascular evidence for a co-occurrence of teeth and baleen in an Oligocene mysticete and the transition to filter-feeding in baleen whales. *Zool. J. Linn. Soc.* **194**, 395–415. (doi:10.1093/zoolinnean/zlab017)

64. Griffiths, M. 1988 The platypus. *Sci. Am.* **258**, 84–91.

65. Pasitschniak-Arts, M. & Marinelli, L. 1998 *Ornithorhynchus anatinus*. *Mamm. Species* **585**, 1–9.

66. Deméré, T. A. & Berta, A. 2008 Skull anatomy of the Oligocene toothed mysticete *Aetiocetus weltoni* (Mammalia; Cetacea): Implications for mysticete evolution and functional anatomy. *Zool. J. Linn. Soc.* **154**, 308–352. (doi:10.1111/j.1096-3642.2008.00414.x)

67. Abzhanov, A., Protas, M., Grant, B. R., Grant, P. R. & Tabin, C. J. 2004 Bmp4 and morphological variation of beaks in Darwin's finches. *Science (80-.).* **305**, 1462–1465. (doi:10.1126/science.1098095)

68. Nabholz, B., Künstner, A., Wang, R., Jarvis, E. D. & Ellegren, H. 2011 Dynamic evolution of base composition: causes and consequences in avian phylogenomics. *Mol Biol Evol* **28**. (doi:10.1093/molbev/msr047)

69. Wang, S., Stiegler, J., Wu, P., Chuong, C. M., Hu, D., Balanoff, A., Zhou, Y. & Xu, X. 2017 Heterochronic truncation of odontogenesis in theropod dinosaurs provides insight into the macroevolution of avian beaks. *Proc. Natl. Acad. Sci. U. S. A.* **114**, 10930–10935.

(doi:10.1073/pnas.1708023114)

70. Hautier, L., Gomes Rodrigues, H., Ferreira-Cardoso, S. & Delsuc, F. 2023 3D models related to the publication: From teeth to pad, tooth loss and development of keratinous structures in sirenians. *MorphoMuseuM J.*

71. Kearse, M. et al. 2012 Geneious Basic: An integrated and extendable desktop software platform for the organization and analysis of sequence data. *Bioinformatics* **28**, 1647–1649. (doi:10.1093/bioinformatics/bts199)

72. Sharko, F. S., Boulygina, E. S., Tsygankova, S. V., Slobodova, N. V., Alekseev, D. A., Krasivskaya, A. A., Rastorguev, S. M., Tikhonov, A. N. & Nedoluzhko, A. V. 2021 Steller's sea cow genome suggests this species began going extinct before the arrival of Paleolithic humans. *Nat. Commun.* **12**, 8–15. (doi:10.1038/s41467-021-22567-5)

73. Edgar, R. C. 2004 MUSCLE: Multiple sequence alignment with high accuracy and high throughput. *Nucleic Acids Res.* **32**, 1792–1797. (doi:10.1093/nar/gkh340)

74. Le Duc, D. et al. 2022 Genomic basis for skin phenotype and cold adaptation in the extinct Steller's sea cow. *Sci. Adv.* **8**, 1–9. (doi:10.1126/sciadv.abl6496)

75. Li, H. 2018 Minimap2: Pairwise alignment for nucleotide sequences. *Bioinformatics* **34**, 3094–3100. (doi:10.1093/bioinformatics/bty191)

FIGURE CAPTIONS

Figure 1 - Ontogenetic evidence of the association of dorsal canaliculi to tooth alveoli, vestigial or not, and dental pad. (A–D) 3D models of the mandibles of sirenian fetuses (A, *Trichechus manatus* NHMUK

669 1865-4-28-9; B, *Dugong dugon* IRSNB 5386, mirror image) and adults (C, *Trichechus manatus*
670 NHMUK 1950-1-23-1; D, *Dugong dugon* NHMUK 2005-51) in lateral views. In fetuses (A and B),
671 arrows indicate the location of vestigial tooth loci (but see also S4). Bone is transparent. Dorsal
672 canaliculi – orange; mental branches – purple; mandibular canal – cyan; teeth – dark blue; tooth alveoli
673 – green. Scale bars: 1 cm.
674
675 **Figure 2 -** Comparison of the internal mandibular morphology in (A) *Trichechus manatus* (NHMUK
676 1885-6-30-2) (B) *Dugong dugon* (NHMUK 2023.66), and (C) *Hydrodamalis gigas* (UMZC C1021)
677 showing the link between dorsal canaliculi, teeth and keratinous pad (same color code as Figure 1;
678 keratinized pad is in yellow). Upper left corner, small mandible silhouettes representing dental
679 replacement systems: green arrows indicate dental drift; red arrows indicate molar loss; yellow lines
680 indicate the position of the keratinous pad. Scale bars: 1 cm.
681
682 **Figure 3 -** Evolution of dorsal canaliculi linked to tooth reduction in five paleogene and four neogene
683 sirenian species (including two extant ones). Timetree (according to [22]) with corresponding 3D
684 reconstructions of the internal mandibular morphology (same color code as Figure 1). Some animal
685 silhouettes are colored in black (extant species and Steller's sea cow). Scale bars: 1 cm. Paintings by
686 Michelle S. Fabros.
687
688 **Figure 4 -** A. Summary of dental gene functionality in three sirenian species and their most recent
689 common ancestors. B. DNA sequence alignments of five dental genes derived from four sirenian
690 genome assemblies, highlighting putative inactivating mutations. Gray bars at the top of whole gene
691 assemblies indicate coding exons. Paintings by Michelle S. Fabros.

SUPPORTING INFORMATION

S1. List of CTscanned specimens and associated information.

S2. 3D models showing the variation of dorsal canaliculi in six manatee mandibles (two juveniles and four adults) in lateral view: A, *Trichechus manatus* NHMUK 1950-1-23-1 (juvenile with dp3-dp5 and molars); B, *T. manatus* NHMUK 1843-3-10-12 (adult with molars only); C, *T. manatus* NHMUK 1864-6-5-1 (adult with molars only); D, *T inunguis* NHMUK 1968-12-19-2 (juvenile with dp3-dp5 and molars); E, *T. senegalensis* NHMUK 1885-6-30-2 (adult with molars only); F, *T. senegalensis* UM V97 (adult with molars only). Bone is transparent. Related to Figures 1 and 2. Orange = dorsal canaliculi; purple = mental branches; cyan = mandibular canal; dark blue = teeth; green = tooth alveoli. Scale bars: 1 cm.

S3. 3D models showing the variation of dorsal canaliculi in eight dugong mandibles (four juveniles and four adults) in lateral view: A, NHMUK 1991-413 (juvenile with dp3-dp5 (m1)); B, NHMUK 1946-8-6-2 (juvenile with dp3-m1); C, NHMUK 2023-66 (juvenile with [dp3] dp4-m1 (m2)); D, 1991-427 (juvenile with di3 dc dp3-m1 (m2)); E, NHMUK 1027g (adult with (di2) [dp5] m1-m3); F, UMZC 2016-2 Ceylon V (adult with m1-m3); G, NHMUK 2005-51 (adult with m1-m3); H, UMZC 2017-3-9 (adult with m2-m3; mirror image). Related to Figures 1 and 2. Bone is transparent. Orange = dorsal canaliculi; purple = mental branches; cyan = mandibular canal; dark blue = teeth; green = tooth alveoli. Scale bars: 1 cm.

S4. 3D models of the skull of a manatee (*Trichechus manatus* NHMUK 1865-4-28-9, A and C) and a dugong (*Dugong dugon* IRSNB 5386, B and D, mirror images) fetuses. A and B, lateral view of the cranium and the mandible; C and D, frontal view of the mandibles. Related to Figures 1 and 2. Arrows indicate the location of vestigial tooth loci. Bone is transparent. Orange = dorsal canaliculi; purple = mental branches; cyan = mandibular canal; dark blue = teeth; green = tooth alveoli. Scale bars: 1 cm.

S5. 3D models of mandibles of extinct sirenians species in lateral view: A, *Prorastomus sirenoides* (NHMUK OR-448976), left mandible; B, *Prorastomus sirenoides* (NHMUK OR-448976), right mandible (mirror image); C, *Libysiren sickenbergi* (NHMUK M82429); D, *Eosiren libyca* (NHMUK); E, *Halitherium taulannense* (MNHN RGHP C0009); F, *Rytiodus capgrandi* (MHNT PAL 2017.8.1); G, *Ribodon limbatus* (NHMUK M7073). Related to Figure 3. Bone is transparent. Orange = dorsal canaliculi; purple = mental branches; cyan = mandibular canal; dark blue = teeth; green = tooth alveoli. Scale bars: 1 cm.

S6. 3D models of mandibles of Steller's sea cows (*Hydrodamalis gigas*) in lateral view: A, NHMUK 2023.67; B, NHMUK 1947-10-21-1; C, UMCZ C1021. Related to Figure 3. Bone is transparent. Orange = dorsal canaliculi; purple = mental branches; cyan = mandibular canal; dark blue = teeth; green = tooth alveoli. Scale bars: 1 cm.

S7. DNA short read mappings for the inactivating mutations in *ACP4*, *AMBN*, and *ODAM*. The only reads shown are those that clearly overlap the inferred inactivating mutations. Paintings by Michelle S. Fabros.

735

736 **S8.** DNA short read mappings for the putative deletion in exon 8 of *MMP20*. The only reads shown are
737 those that clearly overlap the portion of exon 8 that supports the deletion (*Hydrodamalis gigas* reference,
738 left alignment) or the identical location with the exon intact (*Dugong dugon* reference, right alignment).
739 Paintings by Michelle S. Fabros.

740

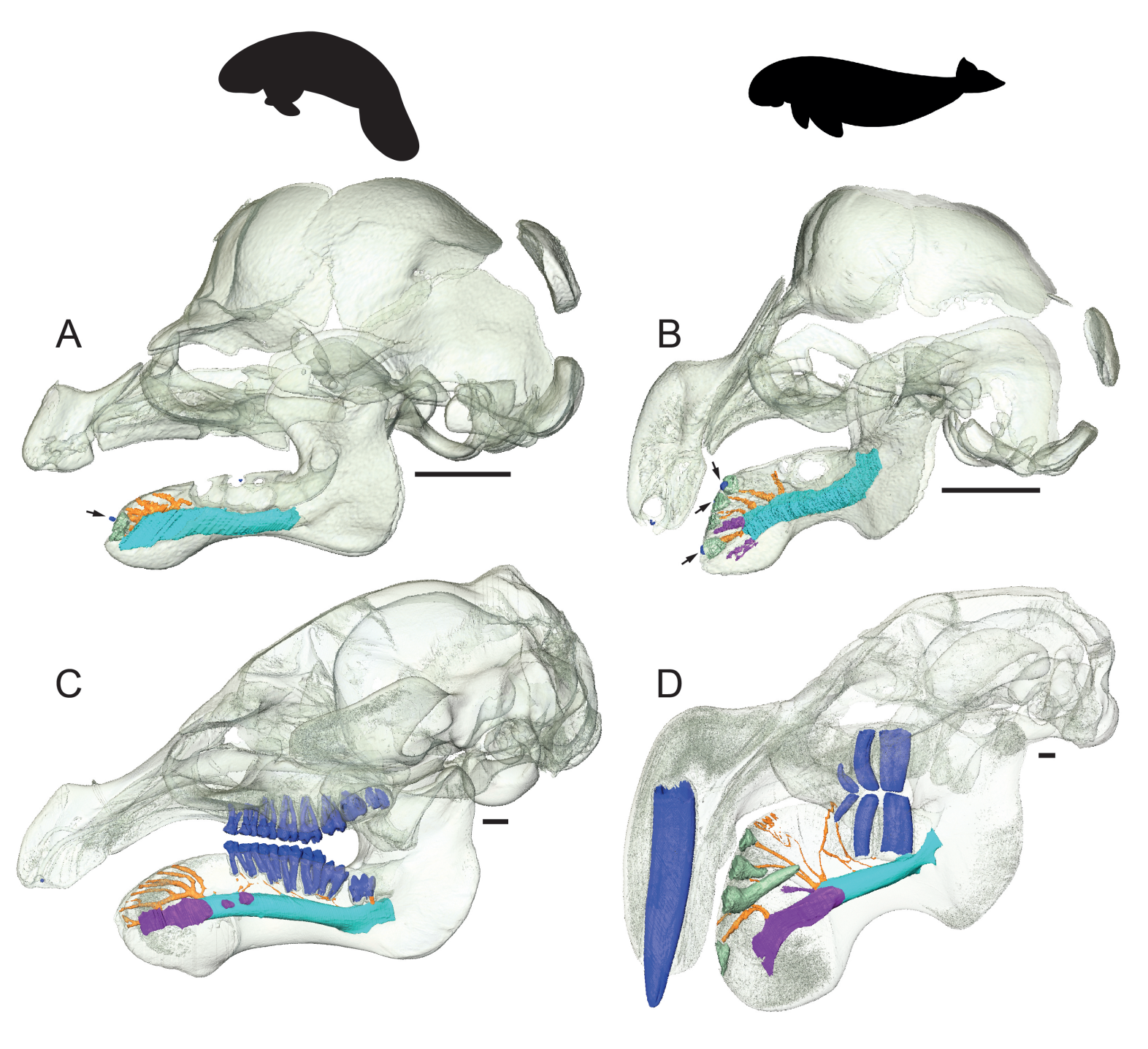
A
B
C
D

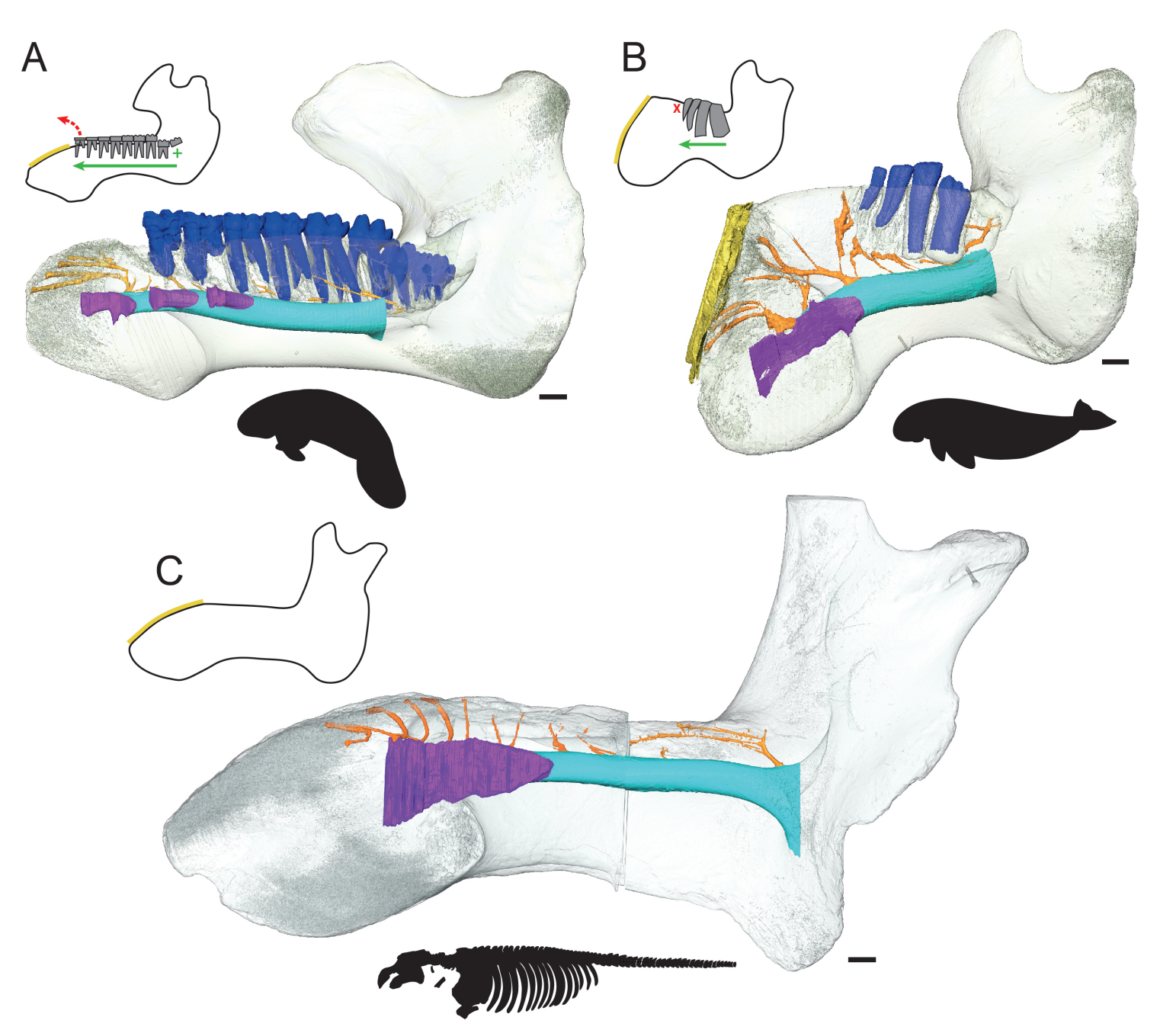
A
B
C

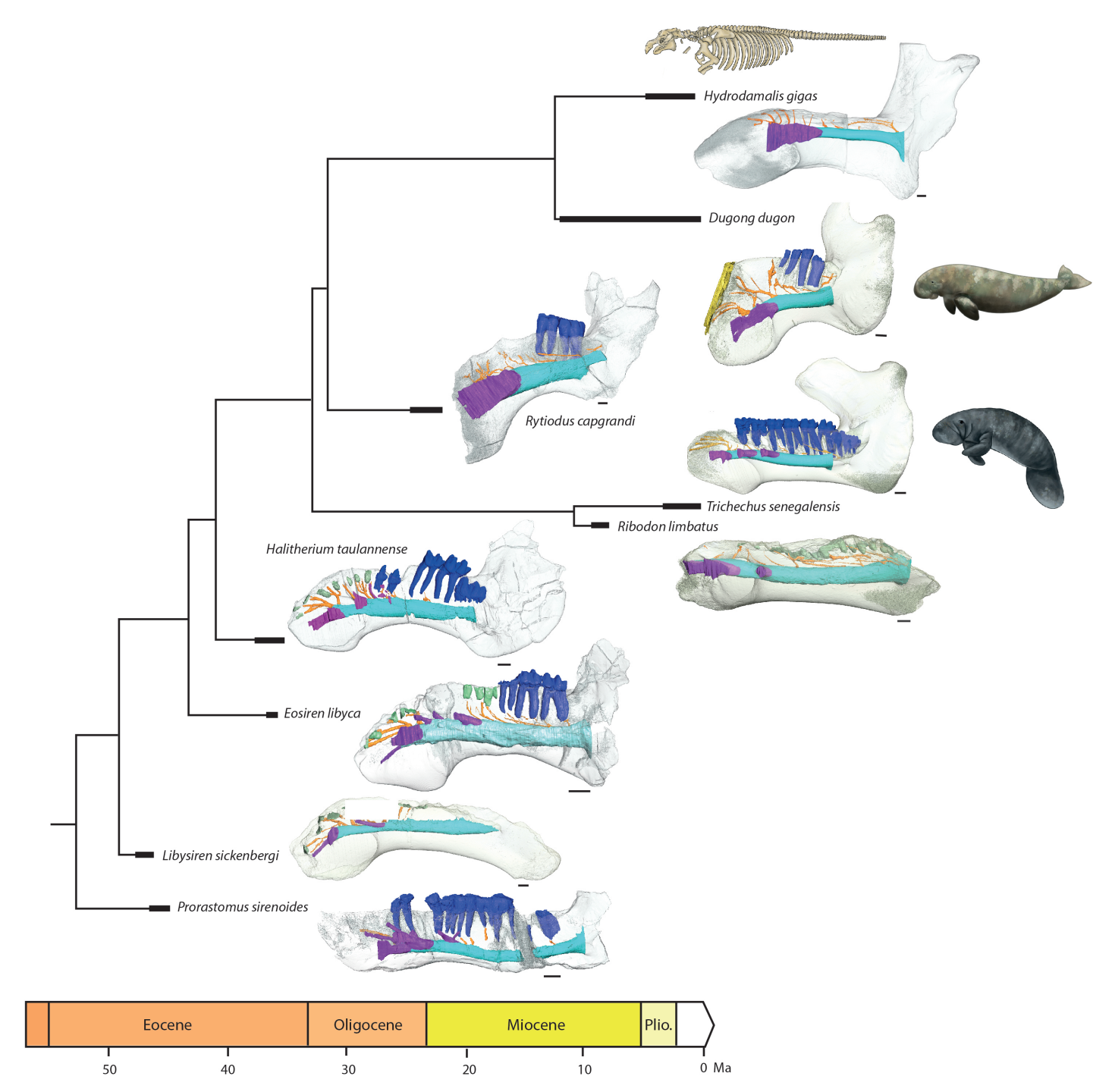
Hydrodamalis gigas
Dugong dugon
Rytiodus capgrandi
Trichechus senegalensis
Ribodon limbatus
Halitherium taulannense
Eosiren libyca
Libysiren sickenbergi
Prorastomus sirenoides
Eocene
Oligocene
Miocene
Plio.
50
40
30
20
10
0 Ma

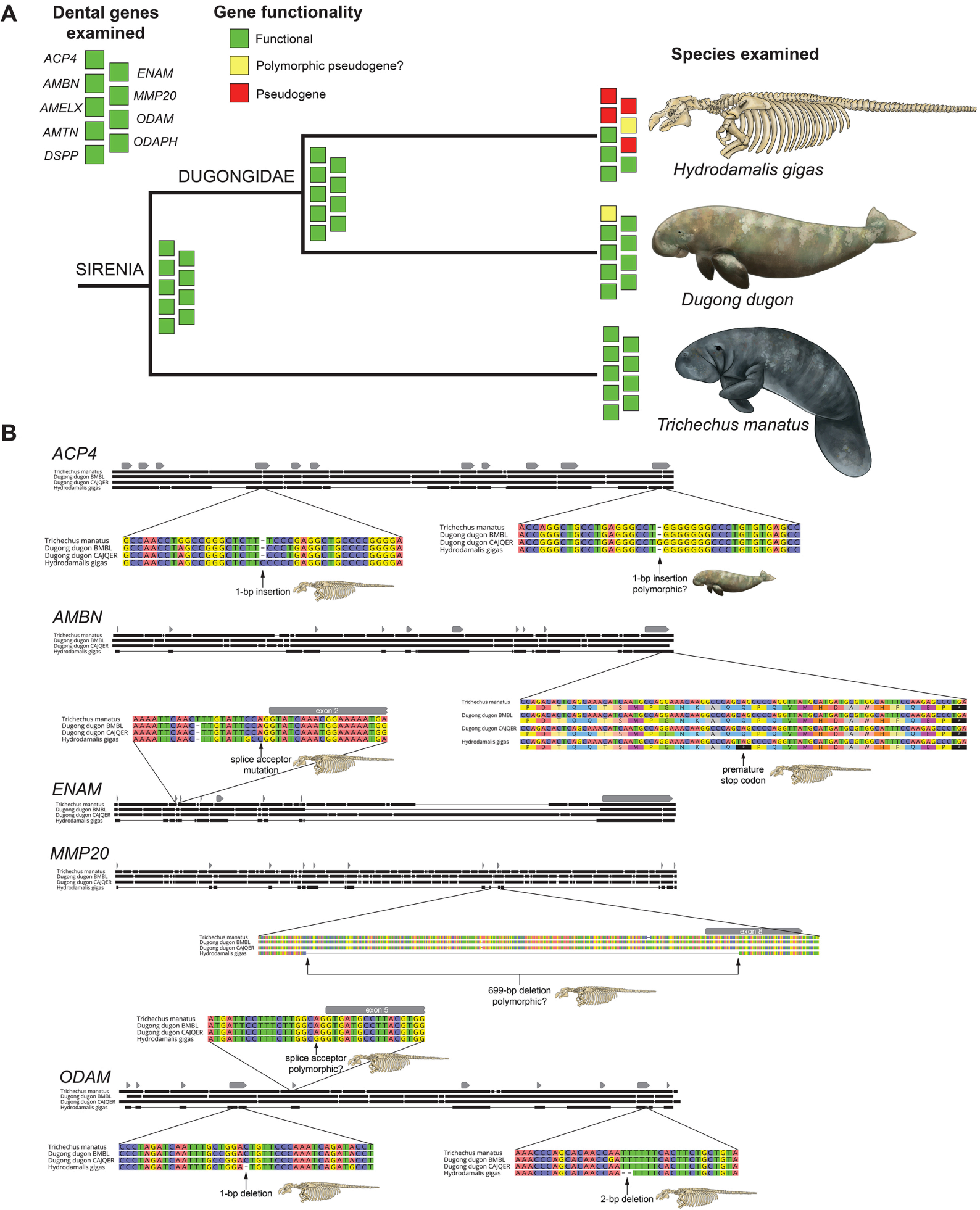
A
Dental genes examined
ACP4
AMBN
AMELX
AMTN
DSPP
ENAM
MMP20
ODAM
ODAPH
Gene functionality
Functional
Polymorphic pseudogene?
Pseudogene
Species examined
DUGONGIDAE
SIRENIA
Hydrodamalis gigas
Dugong dugon
Trichechus manatus
B
ACP4
Trichechus manatus
Dugong dugon BMBL
Dugong dugon CAJQER
Hydrodamalis gigas
1-bp insertion
1-bp insertion polymorphic?
AMBN
exon 2
splice acceptor mutation
premature stop codon
ENAM
MMP20
exon 8
699-bp deletion polymorphic?
exon 5
splice acceptor polymorphic?
ODAM
1-bp deletion
2-bp deletion

Collection	Specimen number	Genus	species	Resolution
NHMUK	1946.8.6.1	*Dugong*	*dugon*	0,112
NHMUK	1946.8.6.2	*Dugong*	*dugon*	0,085
NHMUK	2005.51	*Dugong*	*dugon*	0,123
NHMUK	2005.50	*Dugong*	*dugon*	0.127
NHMUK	1991.427	*Dugong*	*dugon*	0,127
NHMUK	1870.8.16.1	*Dugong*	*dugon*	0,127
NHMUK	1946.8.6.1	*Dugong*	*dugon*	0,127
NHMUK	1991.413	*Dugong*	*dugon*	0,111
NHMUK	2023.68	*Dugong*	*dugon*	0.093
NHMUK	2023.66	*Dugong*	*dugon*	0,127
NHMUK	2023.65	*Dugong*	*dugon*	0.127
NHMUK	1991.404	*Dugong*	*dugon*	0.121
NHMUK	1991.411	*Dugong*	*dugon*	0.112
UMZC	2016-2 Ceylon V	*Dugong*	*dugon*	0,25
UMZC	2017-3-9	*Dugong*	*dugon*	0,25
NHMUK	1848.8.29.7/GERM 1027g	*Dugong*	*dugon*	0,119
IRSNB	5386	*Dugong*	*dugon*	0,077
NHMUK	65.4.28.9	*Trichechus*	*sp.*	0,105
AMNH	53939	Trichechus	sp.	0.5
NHMUK	1852.3.2.3	*Trichechus*	*sp.*	0.062
NHMUK	1864.6.5.1	*Trichechus*	*manatus*	0,123
NHMUK	1963.8.22.1	*Trichechus*	*manatus*	0.115
NHMUK	1950.1.23.1	*Trichechus*	*manatus*	0,122
NHMUK	1843.3.10.12	*Trichechus*	*manatus*	0,101
UM	ISEM V97	*Trichechus*	*manatus*	0,12
NHMUK	1897.2.8.1	*Trichechus*	*inunguis*	0.102
NHMUK	1868.12.19.2	*Trichechus*	*inunguis*	0,08
NHMUK	1894.7.25.8	*Trichechus*	*senegalensis*	0,064
NHMUK	1388f	*Trichechus*	*senegalensis*	0.127
NHMUK	1957.8.21.2	*Trichechus*	*senegalensis*	0.127
NHMUK	1950.7.20.1	*Trichechus*	*senegalensis*	0.127
NHMUK	1885.6.30.2	*Trichechus*	*senegalensis*	0,116
NHMUK	GERM 1388	*Trichechus*	*senegalensis*	0,127
NHMUK	OR.448976	*Prorastomus*	*sirenoides*	0,121
NHMUK	M.45675b	*Libysiren*	*sickenbergi*	0,127
NHMUK	M.82424	*Libysiren*	*sickenbergi*	0,112
NHMUK	M.82428	*Libysiren*	*sickenbergi*	0.104
NHMUK	M.82429	*Libysiren*	*sickenbergi*	0,101
NHMUK	M.10175	*Eosiren*	*libyca*	0,127
NHMUK	1913-22	*Eosiren*	*libyca*	0,12
NHMUK	M.82418	*Rytiodus*	*sp.*	0,118
MHNT	PAL2017-8-1	*Rytiodus*	*capgrandi*	0,094
NHMUK	M.7073	*Ribodon*	*limbatus*	0,115
MNHN	RGHP C001	*Halitherium*	*taulannense*	0,107
MNHN	RGHP C009	*Halitherium*	*taulannense*	0,141
NHMUK	1947.10.21.1	*Hydrodamalis*	*gigas*	0,127
UMZC	C1021	*Hydrodamalis*	*gigas*	0,125
NHMUK	2023.67	*Hydrodamalis*	*gigas*	0,127

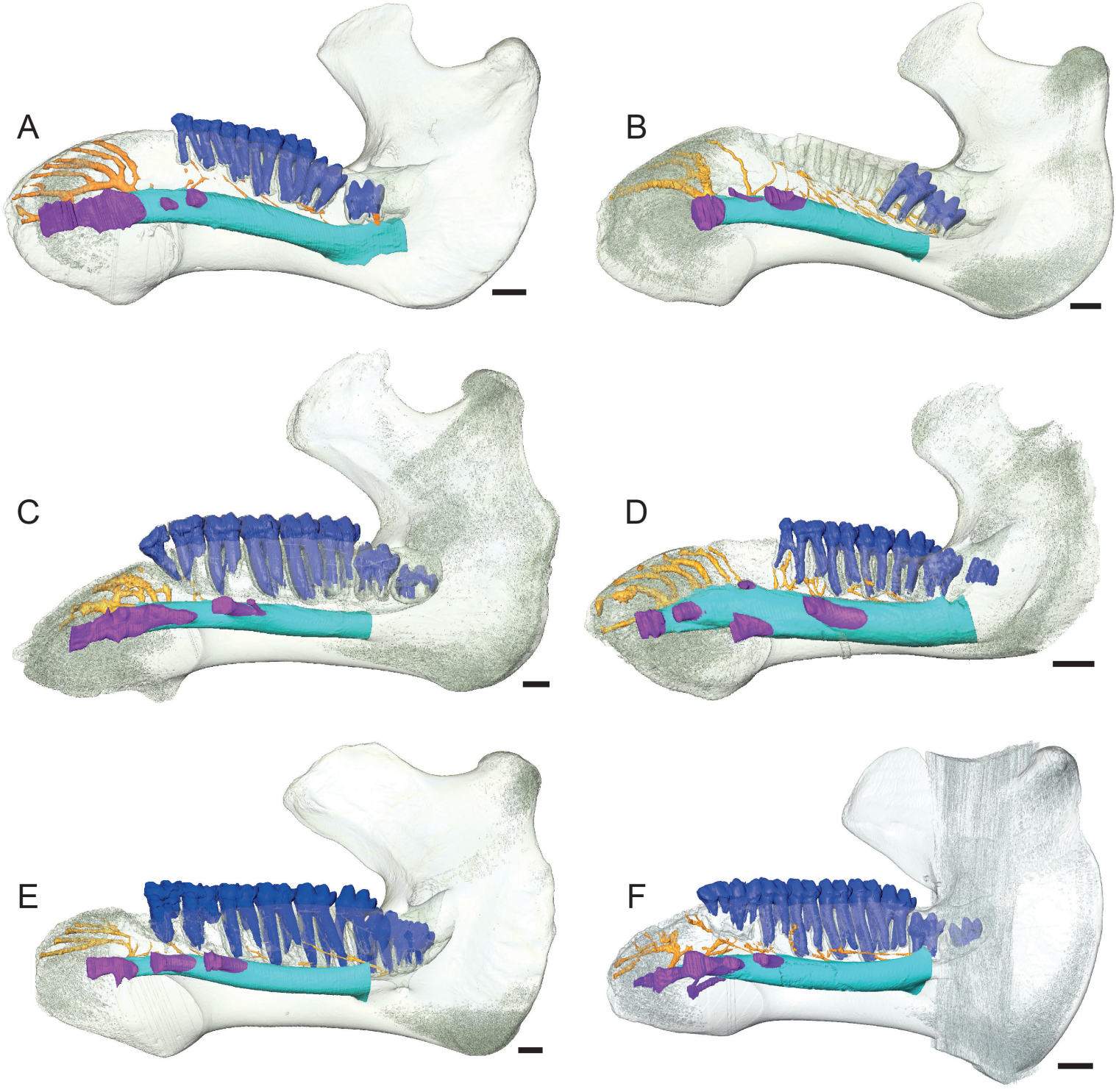
A
B
C
D
E
F

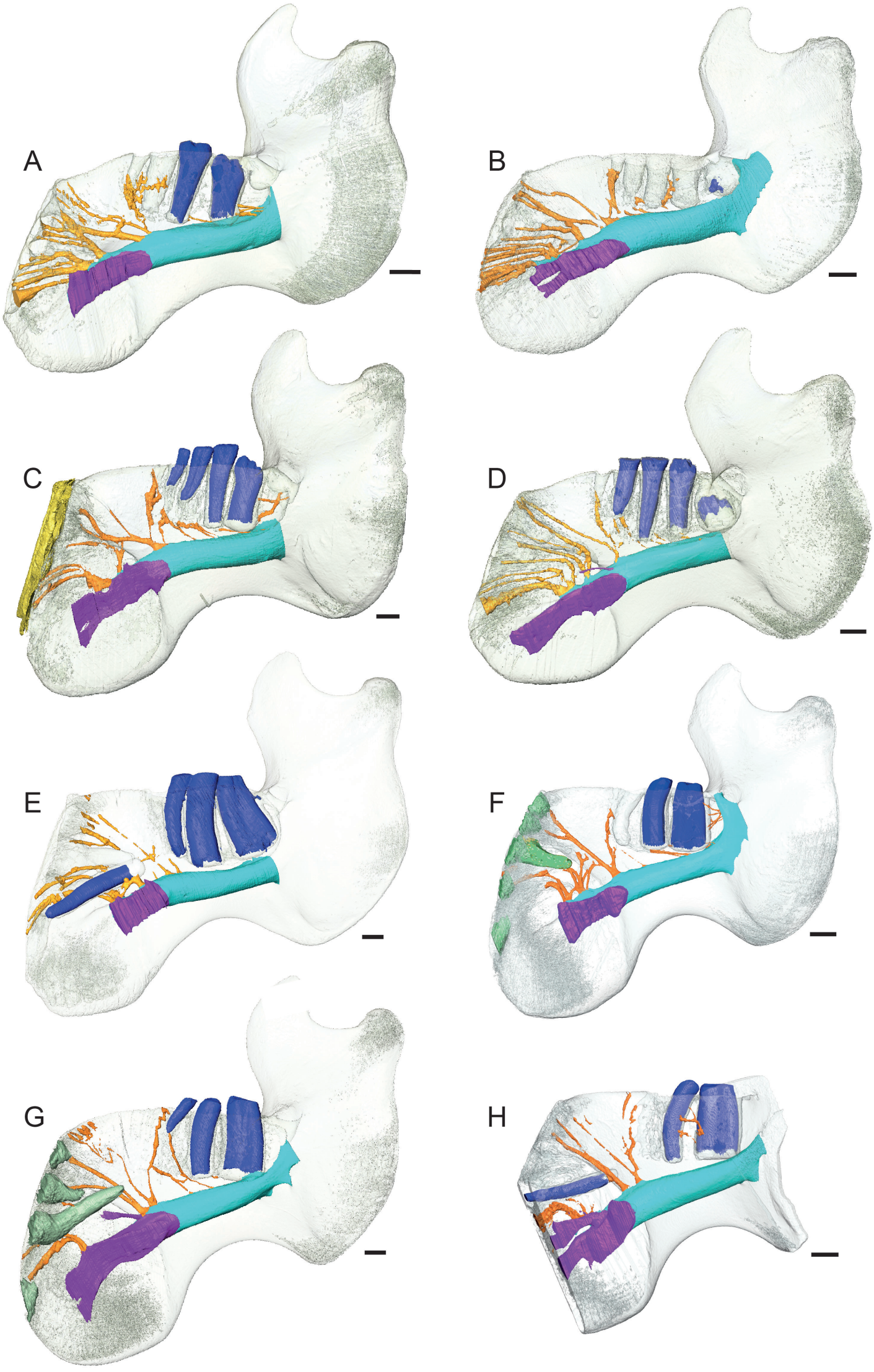
A
B
C
D
E
F
G
H

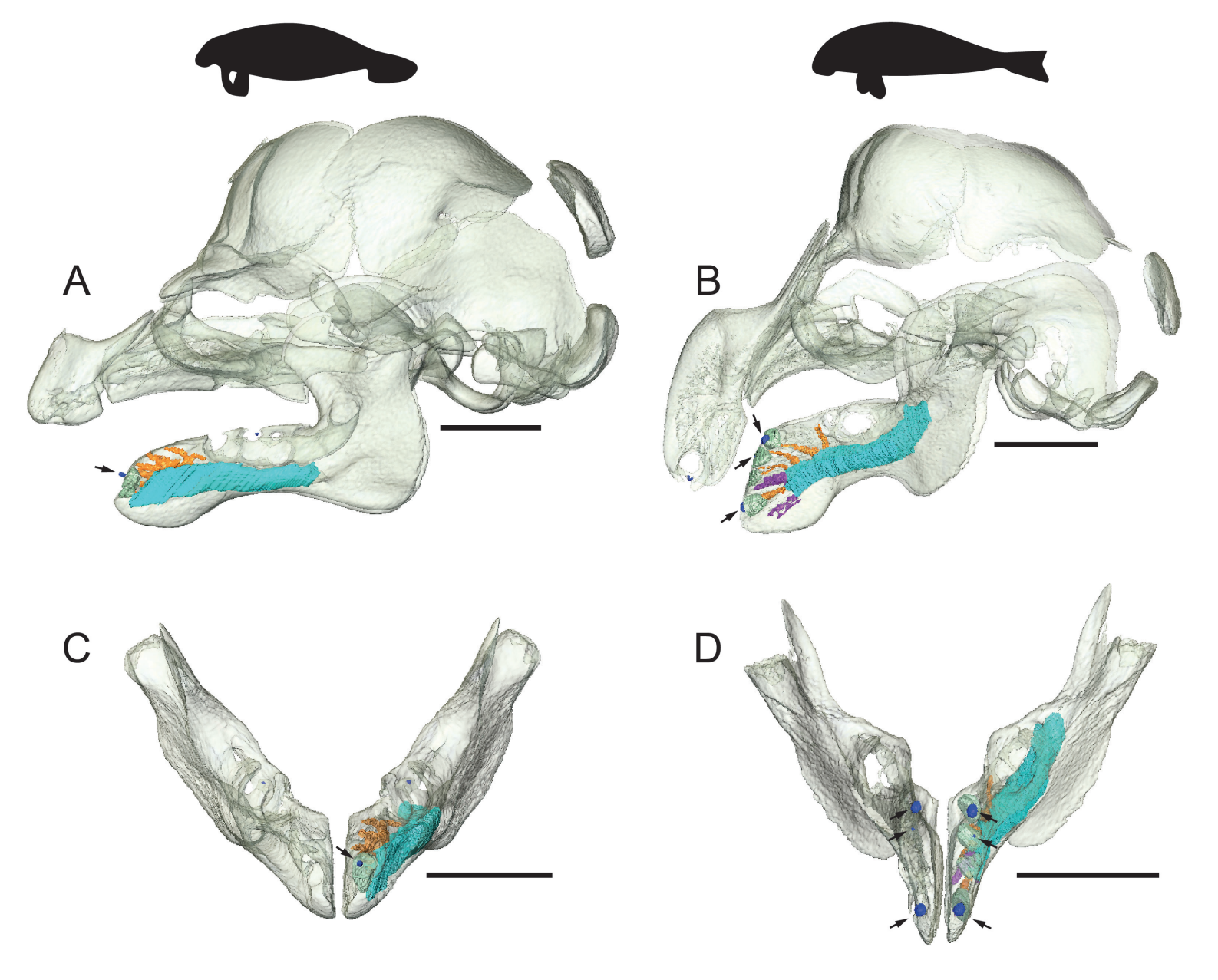
A
B
C
D

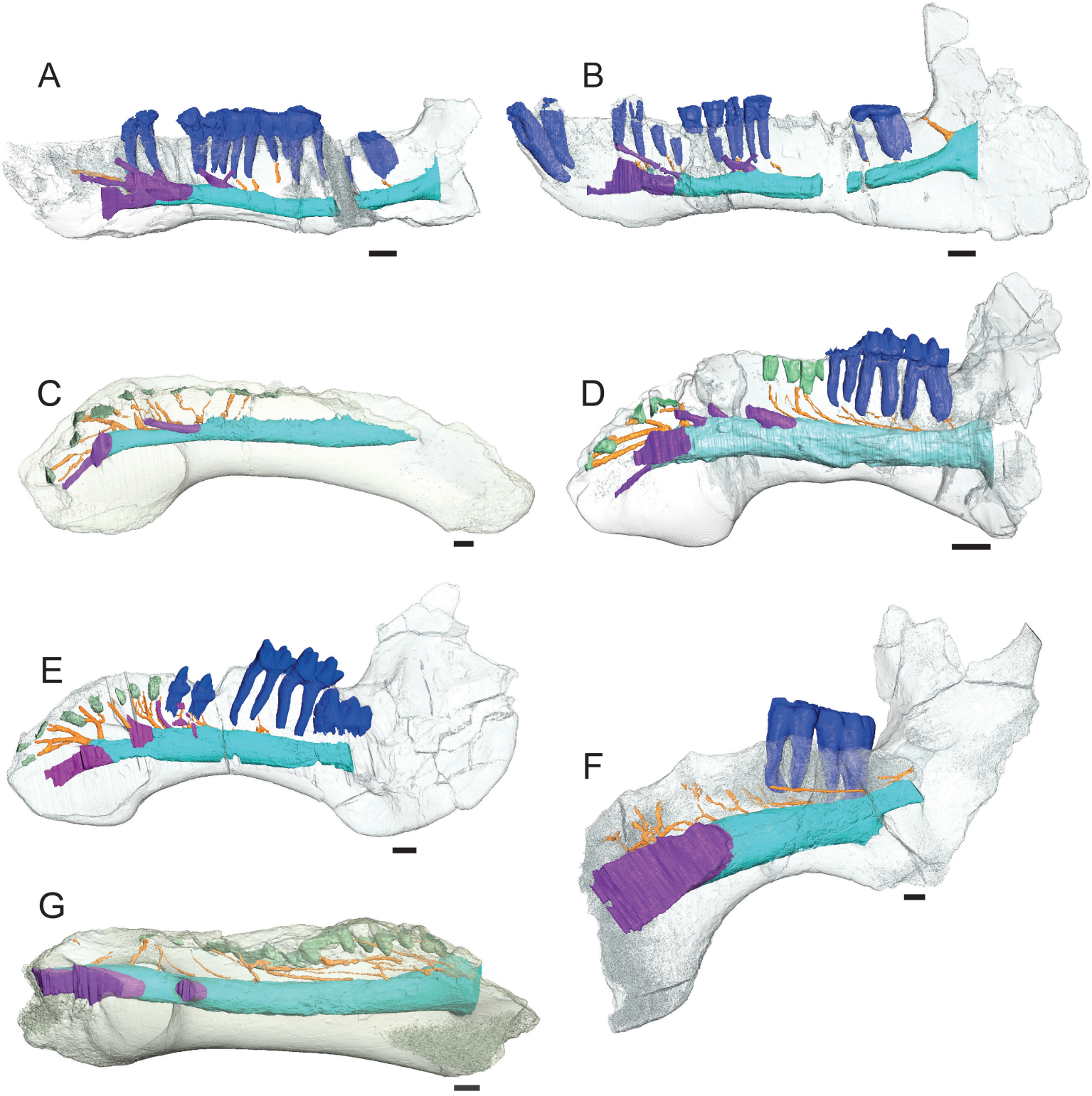
A
B
C
D
E
F
G

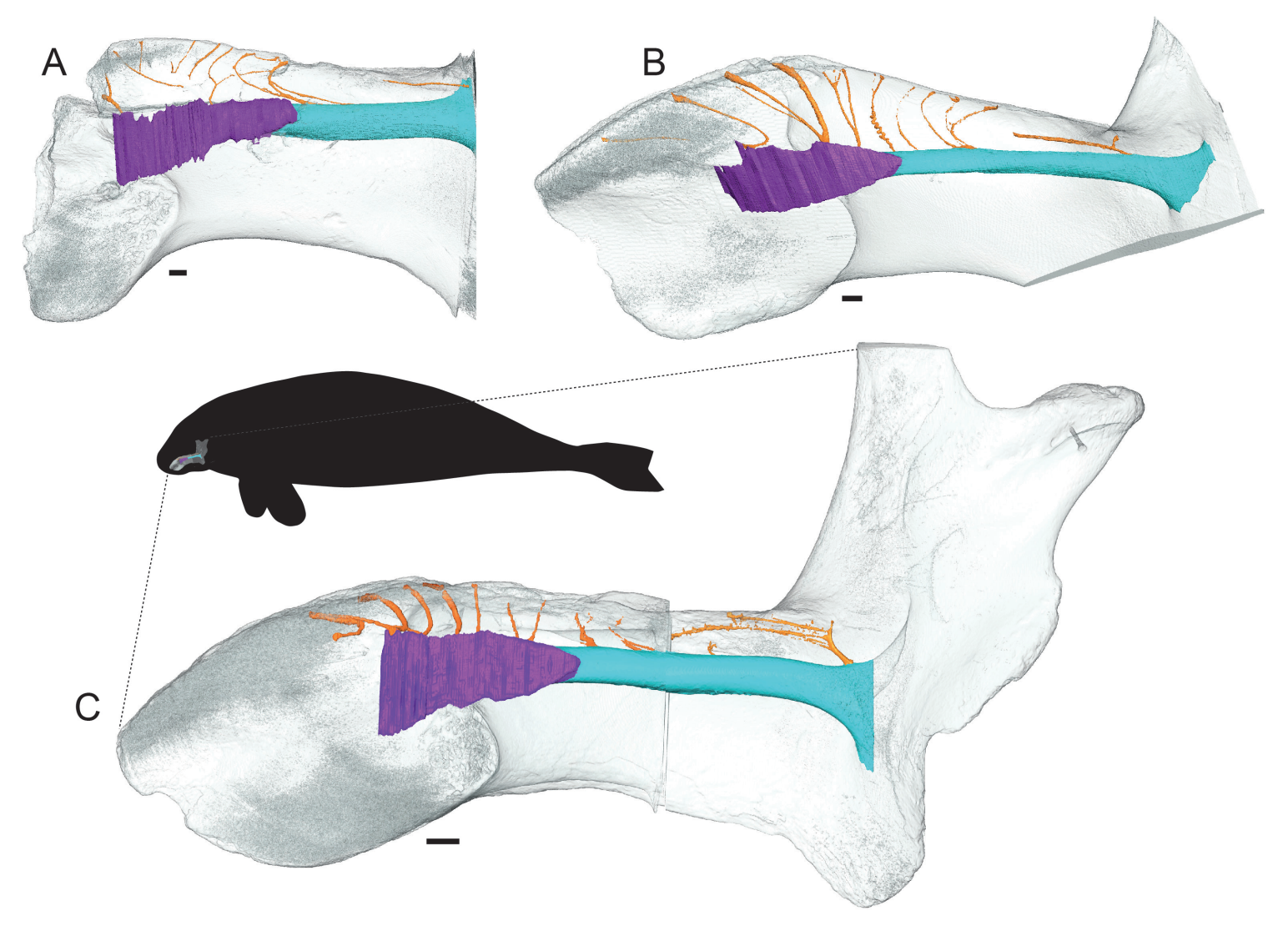
A
B
C

Dugong dugon ACP4 exon 13, 1-bp insertion

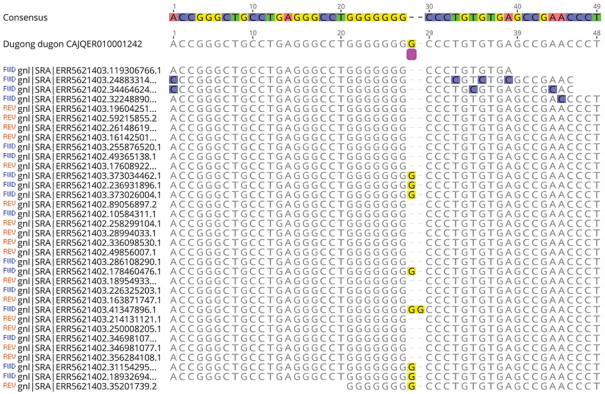

Hydrodamalis gigas ACP4 exon 4, 1-bp insertion

Hydrodamalis gigas ODAM exon 4, 1-bp deletion

Hydrodamalis gigas AMBN exon 13, premature stop codon

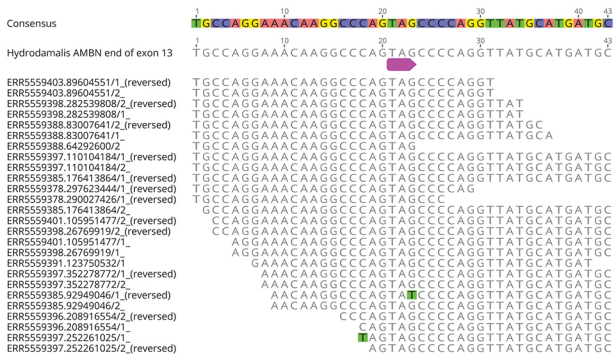

Hydrodamalis gigas ODAM intron 4, splice acceptor mutation

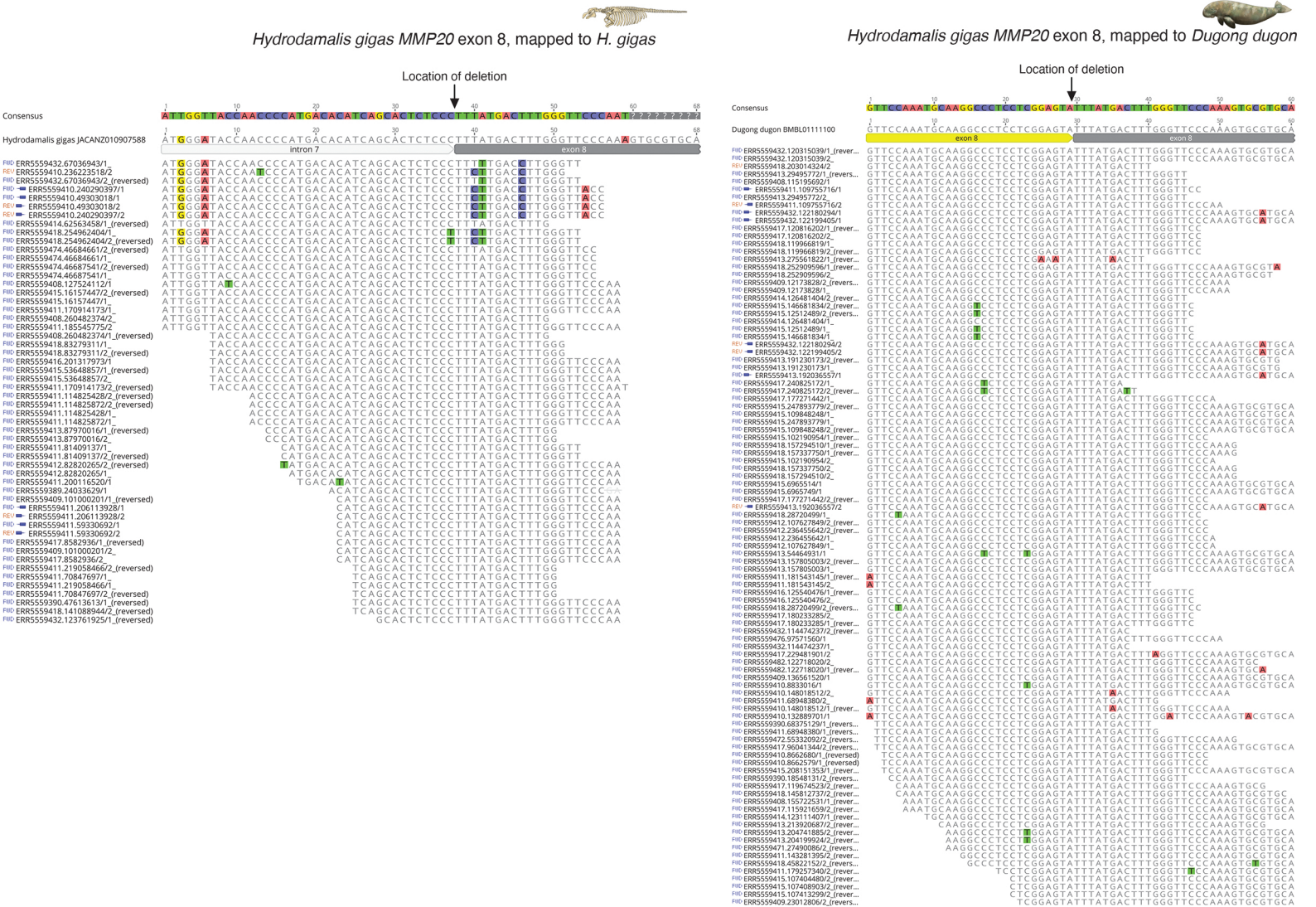
Hydrodamalis gigas MMP20 exon 8, mapped to H. gigas
Location of deletion
Consensus
Hydrodamalis gigas JACANZ010907588
intron 7
exon 8
FWD ERR5559432.67036943/1
REV ERR5559410.236223518/2
FWD ERR5559432.67036943/2_(reversed)
FWD ERR5559410.2402903977/1
FWD ERR5559410.49303018/1
REV ERR5559410.49303018/2
REV ERR5559410.2402903977/2
FWD ERR5559414.62563458/1_(reversed)
FWD ERR5559418.254962404/1
FWD ERR5559418.254962404/2_(reversed)
FWD ERR5559474.46684661/2_(reversed)
FWD ERR5559474.46684661/1_
FWD ERR5559474.46687541/2_(reversed)
FWD ERR5559474.46687541/1_
FWD ERR5559408.127524112/1
FWD ERR5559415.161574472/2_(reversed)
FWD ERR5559415.161574472/1_
FWD ERR5559411.170914173/1_
FWD ERR5559408.260482374/2_
FWD ERR5559411.185545775/2
FWD ERR5559408.260482374/1_(reversed)
FWD ERR5559418.83279311/1_
FWD ERR5559418.83279311/2_(reversed)
FWD ERR5559416.201317973/1
FWD ERR5559415.5364885771/2_(reversed)
FWD ERR5559415.5364885772/2_
FWD ERR5559411.170914173/2_(reversed)
FWD ERR5559411.114825428/2_(reversed)
FWD ERR5559411.114825428/1_
FWD ERR5559411.114825872/1_
FWD ERR5559413.87970016/1_(reversed)
FWD ERR5559413.87970016/2_
FWD ERR5559411.81409137/1_
FWD ERR5559411.81409137/2_(reversed)
FWD ERR5559412.82820265/2_(reversed)
FWD ERR5559412.82820265/1_
FWD ERR5559411.200116520/1
FWD ERR5559389.24033629/1
FWD ERR5559409.1010002201/1_(reversed)
FWD ERR5559411.206113928/1
REV ERR5559411.206113928/2
FWD ERR5559411.59330692/1
REV ERR5559411.59330692/2
FWD ERR5559417.8582936/1_(reversed)
FWD ERR5559409.1010002201/2_
FWD ERR5559417.8582936/2_
FWD ERR5559411.219058466/2_(reversed)
FWD ERR5559411.7084769/71_
FWD ERR5559411.219058466/1_
FWD ERR5559411.7084769/72_(reversed)
FWD ERR5559390.47613613/1_(reversed)
FWD ERR5559418.141088944/2_(reversed)
FWD ERR5559432.123761925/1_(reversed)
Hydrodamalis gigas MMP20 exon 8, mapped to Dugong dugon
Location of deletion
Consensus
Dugong dugon BMBL01111100
exon 8
FWD ERR5559432.120315039/1_(rever...
FWD ERR5559432.120315039/2_
REV ERR5559417.1208162021/2_
FWD ERR5559413.2949577271/1_(revers...
FWD ERR5559408.11519569271
FWD ERR5559411.109755716/1
FWD ERR5559413.2949577272/1
REV ERR5559411.109755716/2
FWD ERR5559432.1221802941/1
FWD ERR5559432.1221990451/1
FWD ERR5559414.1208162021/1_(rever...
FWD ERR5559417.1208162021/2_
FWD ERR5559418.119966819/1_
FWD ERR5559418.119966819/2_(rever...
FWD ERR5559413.2755618222/1_(rever...
FWD ERR5559418.252909596/1_(rever...
FWD ERR5559411.109755716/2
FWD ERR5559409.12173828/2_(revers...
FWD ERR5559409.12173828/1
FWD ERR5559414.1264814041/2_(rever...
FWD ERR5559415.146681834/2_(rever...
FWD ERR5559415.12512489/2_(revers...
FWD ERR5559414.1264814041/1_
FWD ERR5559415.12512489/1
FWD ERR5559415.146681834/1
REV ERR5559432.1221802941/2
REV ERR5559432.1221990451/2
FWD ERR5559413.191230173/2_(rever...
FWD ERR5559413.191230173/1_
FWD ERR5559413.1920365571/1
FWD ERR5559417.240825172/1_
FWD ERR5559417.240825172/2_(rever...
FWD ERR5559417.1772714421/1_
FWD ERR5559415.247893779/2_(rever...
FWD ERR5559415.109848248/2_(rever...
FWD ERR5559415.247893779/1_
FWD ERR5559415.109848248/1_(rever...
FWD ERR5559415.102190954/2_(rever...
FWD ERR5559418.157329750/1_(rever...
FWD ERR5559418.157329750/2_
FWD ERR5559418.157329751/2_
FWD ERR5559418.157329751/1_
FWD ERR5559415.69655141/2_(rever...
FWD ERR5559415.69655749/1
FWD ERR5559417.1772714422/2_(rever...
REV ERR5559413.1920365572/2
FWD ERR5559418.28720499/1_
FWD ERR5559412.107627849/2_(rever...
FWD ERR5559412.236455642/2_(rever...
FWD ERR5559412.236455642/1_
FWD ERR5559412.107627849/1_
FWD ERR5559413.54464931/1
FWD ERR5559413.157805003/2_(rever...
FWD ERR5559413.157805003/1_
FWD ERR5559411.181543145/1_(rever...
FWD ERR5559411.181543145/2_
FWD ERR5559416.125540476/1_(rever...
FWD ERR5559416.125540476/2_
FWD ERR5559418.28720499/2_(rever...
FWD ERR5559417.180233285/2_
FWD ERR5559417.180233285/1_(rever...
FWD ERR5559432.1144742372/2_(rever...
FWD ERR5559476.97571560/1
FWD ERR5559432.1144742371/1_
FWD ERR5559417.2294819012/2
FWD ERR5559482.122718020/2_
FWD ERR5559482.122718020/1_(rever...
FWD ERR5559409.136561520/1
FWD ERR5559410.8833016/1
FWD ERR5559410.1480185212/2_
FWD ERR5559411.68948380/2_
FWD ERR5559410.1480185212/1_(rever...
FWD ERR5559410.132889701/1
FWD ERR5559390.68375129/1_(revers...
FWD ERR5559411.68948380/1_(revers...
FWD ERR5559472.55332092/2_(revers...
FWD ERR5559417.960413442/2_(revers...
FWD ERR5559410.8662680/1_(reversed)
FWD ERR5559410.8662579/1_(reversed)
FWD ERR5559415.208151353/1_(revers...
FWD ERR5559390.18548131/2_(revers...
FWD ERR5559417.1196745232/2_(rever...
FWD ERR5559418.145812737/2_(rever...
FWD ERR5559408.155722531/1_(rever...
FWD ERR5559417.1159216592/2_(rever...
FWD ERR5559414.1231114071/1_(rever...
FWD ERR5559413.213920687/2_(rever...
FWD ERR5559413.204741885/2_(rever...
FWD ERR5559413.204199924/2_(rever...
FWD ERR5559471.274900862/2_(revers...
FWD ERR5559411.143281395/2_(rever...
FWD ERR5559418.458221522/2_(revers...
FWD ERR5559411.179257340/2_(rever...
FWD ERR5559415.107404480/2_(rever...
FWD ERR5559415.107408903/2_(rever...
FWD ERR5559415.107413299/2_(rever...
FWD ERR5559409.230128067/2_(revers...